ASTRONOMY AND ASTROPHYSICS

The ESO Nearby Abell Cluster Survey*

III. Distribution and kinematics of emission-line galaxies

A. Biviano[1,5], P. Katgert[1], A. Mazure[2], M. Moles[3,6], R. den Hartog[1,7], J. Perea[3], and P. Focardi[4]

[1] Sterrewacht Leiden, P.O. Box 9513, 2300 RA Leiden, The Netherlands
[2] IGRAP, Laboratoire d'Astronomie Spatiale, Marseille, France
[3] Instituto de Astrofísica de Andalucía, CSIC, Granada, Spain
[4] Dipartimento di Astronomia, Università di Bologna, Italy
[5] ISO Science Team, ESA, Villafranca, Spain
[6] Observatorio Astronomico Nacional, Madrid, Spain
[7] ESTEC, SA Division, Noordwijk, The Netherlands

Received 6 September 1996 / Accepted 7 October 1996

Abstract. We have used the ESO Nearby Abell Cluster Survey (ENACS) data, to investigate the frequency of occurrence of Emission-Line Galaxies (ELG) in clusters, as well as their kinematics and spatial distribution.

Well over 90% of the ELG in the ENACS appear to be spirals; however, we estimate that the detected ELG represent only about one-third of the total spiral population.

The *apparent* fraction of ELG increases towards fainter magnitude, as redshifts are more easily obtained from emission lines than from absorption lines. From the ELG that have an absorption-line redshift as well, we derive a *true* ELG fraction in clusters of 0.10, while the *apparent* fraction is 0.16.

The *apparent* ELG fraction in the field is 0.42, while the *true* fraction is 0.21. The *true* ELG fractions in field and clusters are consistent if the differences in morphological mix are taken into account. Thus, it is not necessary to assume that ELG in and outside clusters have different emission-line properties.

The average ELG fraction in clusters depends on global velocity dispersion σ_V : the *true* fraction decreases from 0.12 for $\sigma_V \lesssim 600$ km s^{-1} to 0.08 for $\sigma_V \gtrsim 900$ km s^{-1} .

In only 12 out of 57 clusters, the average velocity of the ELG differs by more than 2σ from that of the other galaxies, and in only 3 out of 18 clusters σ_V of the ELG differs by more than 2σ from that of the other galaxies. Yet, combining the data for 75 clusters, we find that σ_V of the ELG is, on average, 20 % larger than that of the other galaxies. It is unlikely that this is primarily due to velocity offsets of the ELG with regard to the other galaxies; instead, the larger σ_V for the ELG must be largely intrinsic.

The spatial distribution of the ELG is significantly less peaked towards the centre than that of the other galaxies. This causes the average projected density around ELG to be $\sim 30\%$ lower than it is around the other galaxies. In combination with the inevitable magnitude bias against galaxies without detectable emission lines, this can lead to serious systematic effects in the study of distant clusters.

From an analysis of the distributions of projected pair distances and velocity differences we conclude that at most 25% of the ELG are in compact substructures, while the majority of the ELG are distributed more or less smoothly.

The virial estimates of the cluster masses based on the *ELG only* are, on average, about 50% higher than those derived from the other galaxies. This indicates that the ELG are either on orbits that are significantly different from those of the other galaxies, or that the ELG are not in virial equilibrium with the other galaxies, or both.

The velocity dispersion profile of the ELG is found to be consistent with the ELG being on more radial orbits than the other galaxies. For the ELG, a ratio between tangential and radial velocity dispersion of 0.3 to 0.8 seems most likely, while for the other galaxies the data are consistent with isotropic orbits.

The lower amount of central concentration, the larger value of σ_V and the possible orbital anisotropy of the ELG, as well as their content of line-emitting gas would be consistent with a picture in which possibly all spirals (but certainly the late-type ones) have not yet traversed the virialized cluster core, and may even be on a first (infall) approach towards the central, high-density region.

Key words: galaxies: clusters of – galaxies: ISM galaxies: kinematics and dynamics – cosmology: observations

Send offprint requests to: P. Katgert

* Based on observations collected at the European Southern Observatory (La Silla, Chile)

1. Introduction

Galaxies of different morphological types live in different environments (e.g. Hubble & Humason 1931). Dressler (1980a) was the first to clearly establish the dependence of the fractions of early- and late-type cluster galaxies on the local galaxy density. The dependence found by Dressler has been verified by many authors, most recently by e.g. Binggeli, Tarenghi & Sandage (1990); Sanromà & Salvador-Solé (1990); Iovino et al. (1993).

Early and late-type cluster galaxies not only differ in their spatial distribution, but also in their kinematics. Moss & Dickens (1977) claimed that the velocity dispersion, $\sigma_{\rm v}$, of the population of late-type galaxies is significantly larger than that of the early-type galaxies, in 4 of the 5 clusters for which they could determine velocity dispersions for early- and late-type galaxies separately. Their study was a follow-up of earlier suggestions that the kinematics of early- and late-type galaxies in the Virgo cluster are different. Differences in average velocity, $<$v$>$ (de Vaucouleurs 1961), as well as in $\sigma_{\rm v}$ (Tammann 1972) had been reported. Only the $\sigma_{\rm v}$ -difference was subsequently confirmed (Binggeli, Tammann, & Sandage 1987). The early claim of Moss & Dickens (1977) was confirmed by Sodré et al. (1989) and Biviano et al. (1992), from data on galaxies in 15 and 37 galaxy clusters respectively.

In clusters, the dependence of the mix of morphological types on local density (i.e. on distance from the cluster center), and the differences in kinematics that are related to this, can generally be understood as the result of the evolution of the galaxy population. Several processes may affect the morphology of a galaxy as it passes through the dense cluster core (e.g. ram pressure, merging, tidal stripping and tidal shaking). These processes are believed to be capable of transforming a star-forming spiral galaxy in a quiescent elliptical or S0. On the other hand, it is possible that regions of high density are, from the start, more conducive to the formation of slowly spinning (early-type ?) galaxies (see e.g. Sarazin 1986, and reference therein). It is likely that clusters form mainly through the collapse of density perturbations (e.g. Gunn & Gott 1972) although it is possible that shear also plays a rôle. If such density perturbations have density profiles that fall with radius, it is natural to expect a time sequence of infalling shells of galaxies. The spirals could then be on infalling orbits, as was convincingly shown to be the case in the Virgo cluster by Tully & Shaya (1984), whereas the ellipticals and S0's would constitute the virialized cluster population.

Some recent findings indicate that the latter scenario may well be too simplistic. On the one hand, Zabludoff & Franx (1993) have found that the early- and late-type galaxies have different average velocities in three out of six clusters studied, while the $\sigma_{\rm v}$'s are not different. On the other hand, Andreon (1994) carefully re-examined galaxy morphologies in the Perseus cluster, and did not find a clear morphology-density relation. If groups of galaxies fall into a cluster anisotropically (as suggested e.g. by van Haarlem & van de Weygaert 1993), this may result in an average velocity of the infalling (spiral?) population that differs from that of the other galaxies in the (core of the) cluster. The resulting substructure could, at the same time, wash out the morphology-density relation.

Previous investigations of emission-line galaxies (ELG) in and outside clusters (Gisler 1978; Dressler, Thompson & Shectman 1985; Salzer et al. 1989; Hill & Oegerle 1993; Salzer et al. 1995) have been mainly limited to the comparison of the relative frequency of ELG in clusters and in the field. These studies have shown that emission lines occur more frequently in the spectra of field galaxies than in cluster galaxies (for elliptical galaxies this was already pointed out by Osterbrock, 1960). It was concluded that this difference cannot totally be the result of the morphology-density relation, in combination with the different mix of early- and late-type galaxies. However, recently the kinematics of the ELG has become a subject of study (e.g. Mohr et al. 1996; Carlberg et al. 1996).

In this paper, we re-examine the evidence for differences between early- and late-type galaxies in clusters, by using the extensive data-base provided by the ENACS (the ESO Nearby Abell Cluster Survey). We analyze the frequency of occurrence of ELG in clusters, as well as their distribution with respect to velocity and position and their kinematics. In Sect. 2 we summarize those properties of the ENACS data-base that are relevant for the present discussion. In Sect. 3 we discuss the fraction of ELG in clusters and in the field. In Sect. 4 and Sect. 5 we study the global kinematics and spatial distribution of the ELG in relation to the non-ELG. In Sect. 6 we discuss correlations between positions and velocities of the ELG and non-ELG. In Sect. 7 we investigate the equilibrium and the orbits of the cluster galaxies, and, finally, in Sect. 8 we discuss the implications of our results for ideas about structure and formation of clusters.

2. The data

2.1. The ESO Nearby Abell Cluster Survey

The ENACS has provided reliable redshifts for 5634 galaxies in the directions of 107 cluster candidates from the catalogue of Abell, Corwin & Olowin (1989), with richness $R_{\rm ACO} \geq 1$ and mean redshift $z \lesssim 0.1$. Redshift estimates are mostly based on absorption lines, but for 1231 galaxies, emission lines were detectable in the spectrum. As described in Katgert et al. (1996, hereafter Paper I), for 62 galaxies the reality of the emission lines is doubtful, as judged from a comparison with the absorption-line redshift (in almost all cases these are galaxies with only one emission line detected in the spectrum). That leaves 1169 galaxies with reliable emission lines. For 586 of these, the redshift is based on both absorption and emission lines, and for the remaining 583 galaxies the redshift estimate is based exclusively on emission lines. The estimated redshift errors range from about 40 to slightly over 100 km/s, with the majority less than 70 km/s. For a detailed description of the characteristics of the ENACS data-base we refer to Paper I.

For almost all of the 5634 galaxies a calibrated R-magnitude estimate is available, from photographic photometry calibrated with CCD-imaging. The R-magnitudes of the galaxies with red-

shifts range from 13 to about 18, although the majority of the galaxies have R-magnitudes brighter than about 17.

For most of the galaxies in this survey we could not obtain a reliable morphological classification because the galaxies were identified on copies of survey plates made with Schmidt telescopes. However, we can identify star-forming (i.e. presumably late-type) galaxies on the basis of the presence of the relevant emission lines in their spectra. The clear *advantage* of selecting galaxies on the presence of spectral lines is that the selection is quite effective out to redshifts of $z = 0.1$, whereas it may already be difficult to reliably determine morphologies of galaxies at a redshift $z \approx 0.05$ (e.g. Andreon 1993). The *disadvantage* of a selection on the basis of detectable emission-lines is that the absence of such lines does not decisively prove a galaxy to be an early-type galaxy. In other words: the class of galaxies without detectable emission lines is likely to contain also late-type galaxies with emission lines that are too faint to be detected, or without emission lines. In the following, we will nevertheless refer to the two galaxy populations as ELG and non-ELG. The ELG can be thought of as an almost pure late-type galaxy population (see Sect. 3.2), whereas the non-ELG are a mix of early- and late-type galaxies (which share the property that they do not have detectable emission lines).

2.2. The definition of redshift systems

The 107 pencil beam redshift surveys cover solid angles with angular diameters between 0.5 and about 1.0 deg. In these 107 redshift surveys, 220 systems were found that are compact in redshift and that contain at least 4 (but often several tens to a few hundred) member galaxies. These systems were identified in redshift space, by using the method of fixed gaps (see Paper I), which separates galaxies within a system (with velocity differences between 'neighbours' less than the chosen gap) from galaxies that do not belong to the system (because the velocity difference with the nearest system member is larger than the chosen gap). For the following discussion we will, in addition, divide the cluster Abell 548 into two components, following the suggestion of Escalera et al. (1994) (which was later confirmed by Davis et al. 1995) because the cluster is clearly bi-modal.

Membership of a given galaxy to a particular system requires that the galaxy has a velocity within the velocity limits of the system as defined with the fixed-gap method. For systems with at least 50 galaxies we applied an additional test for membership which uses both the velocity *and* position (see den Hartog & Katgert 1996; see also Mazure et al. 1996, hereafter Paper II). This second criterion removes 74 galaxies for which the combination of position in the cluster and relative radial velocity makes it unlikely that they are within the turn-around radius of their host system. These 74 'interlopers' occur in only 25 of the systems.

The 'interloper'-test involves an estimate of the mass-profile of the system, and therefore requires the centre of the system. Following den Hartog & Katgert (1996), we have assumed the centre to be (in order of preference): 1) the X-ray center, 2) the position of the brightest cluster member in the cluster core, provided it is at least one magnitude brighter than the second brightest member, and/or less than 0.25 h^{-1} Mpc from the geometric center of the galaxy distribution. If these two methods could not be applied, we determined 3) the position of the peak in the surface density, viz. the position of the galaxy with the smallest distance to its $N^{1/2}$-th neighbour (with N the number of galaxies in the system). In several cases this position differed by more than 0.1 h^{-1} Mpc from that of any of the 3 brightest cluster members. We then used 4) a luminosity weighted average position. If the latter was not nearer than 0.25 h^{-1} Mpc to the geometric center, we used 5) the geometric center, as defined by the *biweight* averages of the galaxy positions (see, e.g., Beers, Flynn, & Gebhardt 1990). For 22 of the 25 systems with at least 50 galaxies, the position of the X-ray peak or that of the brightest cluster member were chosen as cluster centers.

2.3. The various samples of Galaxy systems

Our discussion of the differences between the average velocities of ELG and non-ELG within individual clusters will only be based on the 58 systems that contain at least 5 ELG: we consider this a minimum number for the estimation of a meaningful average velocity. In general, such systems also contain at least 5 non-ELG. However, for A3128 ($z = 0.077$), the number of non-ELG is less than 5 and we have therefore not considered it in the analysis for individual systems. That leaves a sample of 57 systems (sample 1) with both at least 5 ELG *and* 5 non-ELG.

In discussing velocity dispersions of *individual* systems we have limited ourselves to the subset of 18 systems with at least 10 ELG (all of which also have at least 10 non-ELG). I.e. we applied a lower limit to the ELG population that is identical to the one used in Paper II, in the discussion of the distribution of velocity dispersions of a complete volume-limited sample of rich clusters. The same restriction was applied in estimating projected harmonic mean radii: from numerical modeling we find that such estimates are biased if they are based on less than 10 positions. The sample of 18 systems with at least 10 ELG will be referred to as sample 2.

Finally, we will also discuss results for a sample of 75 systems with at least 20 members (sample 3). The requirement that the total number of galaxies in a system be at least 20 ensures that the centre of the system can be determined with sufficient accuracy. This sample also defines a 'synthetic' average cluster, which contains 3729 galaxies of which 559 are ELG.

In Table 1 we list some characteristics of all 87 systems in the 3 samples defined above, as well as of the 33 systems with a total number of members from 10 to 19, of which less than 5 are ELG. The total number of galaxies in these 120 systems is 4333, of which 809 are ELG. In col.(1) the ACO number (Abell et al. 1989) of the (parent) ACO system is given, and in col.(2) the average redshift of the system. Col.(3) gives the position of the centre of the system (B1950.0). The number of member galaxies, and the number of member ELG among these are given in col.(4) (note that these numbers do not include the 74 interlopers), and col.(5) lists the projected distance, r_{max}, in h^{-1} Mpc , of the galaxy farthest from the cluster centre.

Table 1. The data-set of 120 systems

Abell	$< z >$	Center	N, N_{ELG}		r_{max}
		α δ			Mpc
		B1950			
13	0.094	00:11:02 –19:45.7	37	3	1.6
87	0.055	00:40:13 –10:04.3	27	2	0.6
118	0.115	00:52:52 –26:37.3	30	8	1.3
119	0.044	00:53:45 –01:31.6	101	5	1.2
151	0.041	01:06:27 –16:12.7	25	5	0.8
151	0.053	01:06:22 –15:40.4	46	10	1.6
151	0.099	01:06:08 –15:53.3	35	5	2.0
168	0.045	01:12:35 +00:01.4	76	6	1.1
229	0.113	01:36:44 –03:53.1	32	8	1.3
295	0.043	01:59:44 –01:22.1	30	1	0.5
367	0.091	02:34:18 –19:35.2	27	3	1.1
380	0.134	02:41:60 –26:26.3	25	4	1.8
420	0.086	03:06:56 –11:46.8	19	5	1.2
514	0.071	04:46:21 –20:37.3	81	11	1.7
524	0.056	04:55:42 –19:45.1	10	2	0.7
524	0.078	04:55:40 –19:47.0	26	12	0.9
543	0.085	05:29:19 –22:19.8	10	1	0.7
548W	0.042	05:43:34 –25:53.3	120	24	1.6
548E	0.041	05:46:38 –25:29.3	114	38	1.5
548	0.087	05:43:36 –25:28.8	14	8	4.6
548	0.101	05:43:47 –25:42.4	21	6	3.1
754	0.055	09:06:49 –09:28.8	39	0	0.8
957	0.045	10:11:08 –00:41.3	34	1	0.6
978	0.054	10:17:56 –06:16.5	61	7	1.5
1069	0.065	10:37:14 –08:25.8	35	0	0.8
1809	0.080	13:50:36 +05:23.6	30	0	0.9
2040	0.046	15:10:21 +07:36.7	37	3	0.6
2048	0.097	15:12:50 +04:34.0	25	1	1.2
2052	0.035	15:14:18 +07:12.4	35	2	0.4
2353	0.121	21:31:47 –01:47.9	24	4	1.4
2361	0.061	21:36:08 –14:32.3	24	7	0.9
2362	0.061	21:37:31 –14:27.5	17	5	1.1
2401	0.057	21:55:36 –20:20.6	23	1	0.6
2426	0.088	22:11:19 –10:24.0	11	0	1.4
2426	0.098	22:11:52 –10:37.4	15	1	1.0
2436	0.091	22:17:59 –03:04.9	14	0	1.1
2480	0.072	22:43:18 –17:53.3	11	1	0.8
2500	0.078	22:50:48 –25:49.3	12	6	0.8
2500	0.090	22:51:03 –25:46.0	13	4	0.8
2569	0.081	23:14:54 –13:05.7	36	2	1.2
2644	0.069	23:38:18 –00:11.1	12	0	1.2
2715	0.114	00:00:12 –34:57.3	14	1	1.3
2717	0.049	24:00:40 –36:12.9	40	2	1.3
2734	0.062	00:08:50 –29:07.9	77	1	1.7
2755	0.095	00:15:11 –35:28.7	22	3	1.2
2755	0.121	00:16:19 –35:25.4	10	2	1.6
2764	0.071	00:18:08 –49:29.4	19	3	1.0
2765	0.080	00:19:01 –21:02.1	16	9	0.9
2778	0.102	00:26:25 –30:26.6	17	9	1.6
2778	0.119	00:25:22 –30:33.7	10	5	1.5
2799	0.063	00:35:02 –39:24.3	36	5	0.8
2800	0.064	00:35:29 –25:20.9	34	6	1.0

Table 1. (continued)

Abell	$< z >$	Center	N, N_{ELG}		r_{max}
		α δ			Mpc
		B1950			
2819	0.075	00:43:46 –63:49.0	49	6	1.4
2819	0.087	00:43:54 –63:52.2	43	6	1.9
2819	0.160	00:41:46 –64:11.8	13	1	4.8
2854	0.061	00:58:34 –50:48.2	22	4	0.8
2871	0.114	01:05:52 –37:01.6	14	3	1.2
2871	0.123	01:05:31 –36:59.4	18	4	1.4
2911	0.081	01:23:51 –38:13.5	31	2	1.0
2923	0.072	01:30:03 –31:20.9	16	3	0.8
3009	0.065	02:20:17 –48:47.5	12	3	0.8
3093	0.083	03:09:15 –47:35.1	22	5	0.9
3094	0.067	03:09:49 –27:09.9	66	16	1.5
3094	0.139	03:09:19 –27:16.9	12	1	3.2
3111	0.078	03:15:55 –45:51.8	35	3	1.0
3112	0.075	03:16:13 –44:24.9	67	16	1.5
3112	0.132	03:16:15 –44:26.8	14	1	2.3
3122	0.064	03:20:21 –41:31.4	89	18	1.7
3122	0.150	03:20:01 –42:03.5	10	2	2.1
3128	0.039	03:29:52 –52:36.3	12	1	1.5
3128	0.060	03:29:27 –52:40.7	152	30	2.4
3128	0.077	03:28:27 –53:13.9	11	7	3.0
3141	0.105	03:34:55 –28:11.0	15	0	1.2
3142	0.066	03:34:35 –39:53.3	12	3	1.1
3142	0.103	03:34:56 –39:57.9	21	2	1.1
3151	0.068	03:38:22 –28:50.2	38	6	0.8
3158	0.059	03:41:38 –53:47.5	105	9	1.7
3194	0.097	03:57:11 –30:18.7	32	8	1.3
3202	0.069	03:59:24 –53:49.3	27	4	0.9
3223	0.060	04:06:34 –30:57.2	73	6	1.5
3341	0.038	05:23:40 –31:35.0	63	11	0.8
3341	0.078	05:22:32 –31:39.6	15	4	1.7
3341	0.115	05:21:42 –31:43.0	18	1	4.0
3354	0.059	05:33:04 –28:34.2	57	10	1.5
3365	0.093	05:46:14 –21:56.5	32	5	1.0
3528	0.054	12:51:41 –28:45.2	28	0	1.1
3558	0.048	13:25:08 –31:14.3	73	9	1.5
3559	0.047	13:27:04 –29:15.4	39	10	1.6
3559	0.113	13:24:59 –29:08.4	11	1	2.9
3562	0.048	13:30:48 –31:24.9	116	21	2.2
3651	0.060	19:48:10 –55:11.4	78	8	1.9
3667	0.056	20:08:27 –56:58.6	103	9	1.8
3682	0.092	20:25:59 –37:07.8	10	1	0.9
3691	0.087	20:30:55 –38:12.7	33	2	1.0
3693	0.091	20:31:15 –34:48.1	16	5	1.2
3695	0.089	20:31:33 –35:59.4	81	9	1.9
3696	0.088	20:32:23 –35:09.8	12	0	1.2
3703	0.073	20:35:53 –61:30.7	18	5	0.9
3703	0.091	20:35:59 –61:25.7	13	2	1.3
3705	0.090	20:38:54 –35:23.9	29	3	1.0
3733	0.039	20:59:01 –28:15.4	41	6	0.6
3744	0.038	21:04:30 –25:37.8	66	13	1.1
3764	0.076	21:22:48 –34:56.9	38	10	0.9
3795	0.089	21:35:54 –32:17.9	13	3	1.3

Table 1. (continued)

Abell	$< z >$	Center	N, N_{ELG}		r_{max}
		α δ			Mpc
		B1950			
3799	0.045	21:36:36 –72:51.9	10	4	0.6
3806	0.076	21:42:50 –57:31.0	97	23	2.3
3809	0.062	21:43:49 –44:07.8	89	21	1.7
3809	0.110	21:46:38 –43:58.5	10	4	3.9
3809	0.142	21:42:20 –44:03.0	11	1	4.5
3822	0.076	21:50:34 –58:06.2	84	15	1.9
3825	0.075	21:55:06 –60:34.3	59	4	1.7
3825	0.104	21:53:39 –60:27.5	17	7	1.9
3827	0.098	21:58:26 –60:10.8	20	1	1.6
3864	0.102	22:16:58 –52:43.0	32	6	1.2
3879	0.067	22:24:05 –69:16.7	45	9	1.5
3897	0.073	22:36:30 –17:36.1	10	0	1.0
3921	0.093	22:46:41 –64:41.7	32	7	1.4
4008	0.055	23:27:49 –39:33.5	27	3	0.7
4010	0.096	23:28:34 –36:47.2	30	6	1.2
4053	0.072	23:52:11 –27:57.6	17	5	0.7

If there are several systems along the line-of-sight to a given cluster, these are identified by their average redshift, which was obtained using the biweight estimator. Throughout this paper, averages are determined with the biweight estimator, since this is statistically more robust and efficient than the standard mean in computing the central location of a data-set (see Beers et al. 1990). When at least 15 velocities are available, velocity dispersions were also computed with the biweight estimator; however, for smaller number of redshifts we used the gapper estimator. These estimators yield the best robust estimates of the true values of location and scale of a given data-set, particularly when outliers are present.

2.4. The emission-line galaxies

In the wavelength range covered by the ENACS observations, and for the redshifts of the clusters studied, the principal emission lines that are observable are [OII] (3727 Å), Hβ (4860 Å) and the [OIII] doublet (4959, 5007 Å). Note that because of the small aperture of the Optopus fibers (2.3 arcsec diameter), we have only sampled emission-lines in the very central regions of the galaxies. For the redshifts of our clusters the diameters of these regions are 2.5 $\pm$ 0.8 h^{-1} kpc . This should be kept in mind when making comparisons with other datasets for which the information about emission lines may refer to much larger or smaller apertures.

The emission lines were identified independently by two of us, in two different ways; first by examining the 2 - D Optopus CCD frames, and second by inspecting the uncleaned wavelength-calibrated 1-D spectra. Two lists of candidate ELG were thus produced, and for the relatively small number of cases in which there was no agreement, both the 2-D frames and 1-D spectra were examined again. The inspection of the 2-D frames allowed easy discrimination against cosmic-ray events (emission lines are soft and round as they are images of the fiber), and against sky-lines (since these are found at the same wavelength in all spectra). While examining the 1-D spectra we also obtained the wavelengths of the emission lines by fitting Gaussians superposed on a continuum to them.

The combined list of galaxies that show emission lines contains 1231 ELG. As mentioned earlier, for 62 of these we have good evidence that the emission line(s) are not real; in the large majority of these cases there is only one line. For a subset of 586 of the remaining 1169 ELG, the reality of the emission lines is borne out by the very good agreement between the absorption- and emission-line redshifts (see Paper I). For the other 583 ELG, no confirmation of the reality of the lines is available; we expect that in at most 10% of these cases the lines are not real.

Among the 1169 ELG there are 78 active galactic nuclei (AGN). These were identified either through the large velocity-width of the Hβ line, or through the intensity ratios of the [OIII] and Hβ lines, and the relative intensity of the [OII] line (if present). We are convinced that our criteria were sufficiently strict that all 78 galaxies that we classify as AGN are indeed *bona fide* AGN. However, at the same time, our criteria were probably too strict to identify all AGN in our dataset.

It should be realized that our ELG sample is not complete with regard to a well-defined limit in equivalent width of the various emission lines. Furthermore, the poorly-defined limit in equivalent width is probably not sufficiently low that essentially all galaxies with emission lines will have been identified as ELG. Therefore, the sample of non-ELG is very likely to contain a mix of real non-ELG (i.e. galaxies without emission-lines) and unrecognized ELG with emission lines that are too weak to be detected in the ENACS observations. Any difference between ELG and non-ELG that we may detect is therefore probably a reduced version of a real difference. For the same reason, the absence of an observable difference between ELG and non-ELG does not prove conclusively that there is no difference between the ELG and the other galaxies.

2.5. Completeness with regard to apparent magnitude

As was discussed in Paper I, spectroscopy was attempted for all galaxies in the fields of the target ACO clusters down to well-defined limits in isophotal magnitude. However, the success rate of the determination of an *absorption-line* redshift depends strongly on the signal-to-noise ratio in the galaxy spectrum. This in turn depends primarily on the surface brightness of that part of the galaxy that illuminates the fibre entrance. As a result, the success rate is highest for intermediate magnitudes, and decreases somewhat for brighter galaxies (as those are large, so that only a small fraction of the total flux is sampled), and quite noticeably for fainter galaxies for which the *total* flux is smaller. On the contrary, the succes rate for the detection of emission lines does not appear to depend significantly on the brightness of the galaxy. Therefore, the relative distribution with regard to magnitude of ELG and non-ELG can be different, as it is

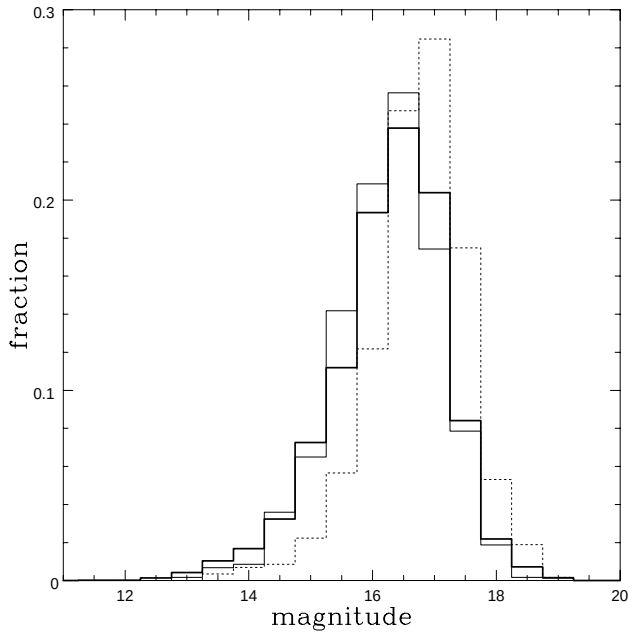

Fig. 1. The normalized distribution with regard to apparent magnitude (R_{25}) for three subsets of the ENACS: the 4447 galaxies with redshift based solely on absorption lines (heavy-line histogram), the 585 galaxies with redshift based both on absorption and emission lines (solid line histogram), and the 583 galaxies with redshift based solely on one or more emission lines (dotted-line histogram).

generally easier to obtain a redshift for a faint galaxy if it has emission-lines in its spectrum, than if it has not.

This is illustrated in Fig. 1 where we show the apparent magnitude distribution of the 4447 galaxies with redshifts determined only from absorption lines, of the 585 galaxies with redshifts determined using both absorption and *emission lines*, and of the 583 galaxies for which the redshift is based only on emission lines (for 19 of the 5634 galaxies magnitudes are not available). The magnitude distribution of the galaxies with redshift based on *emission lines only* is significantly different from the other two (with $>$ .999 probability, according to a Kolmogorov-Smirnov test, see e.g. Press et al. 1986). This figure clearly illustrates the fact that at faint magnitudes it is generally more difficult to obtain a redshift from absorption lines than from emission lines.

From Fig. 1 it is clear that the apparent fraction of ELG varies considerably with magnitude. When calculating the intrinsic ELG fraction one must take this magnitude bias into account (see also Sect. 3.1). However, the magnitude bias is unlikely to be relevant in the analysis of the kinematics and the space distribution of ELG and non-ELG. Since it has been established that velocities and projected clustercentric distances are only very mildly correlated with magnitude (see, e.g., Yepes, Dominguez-Tenreiro & del Pozo-Sanz 1991, and Biviano et al. 1992, and references therein), it seems safe to assume that the different magnitude distributions of ELG and non-ELG will not affect our analysis of the observed space distribution and kinematics.

The magnitude bias in Fig. 1 could affect distributions of clustercentric distance if in the ENACS the magnitude limit would vary with distance from the cluster center. However, when we compare the catalogues of cluster galaxies for which we obtained an ENACS redshift with the (larger) catalogues of *all* galaxies brighter than our magnitude limit (see Paper I), we find that no bias is present. In other words: in all clusters that we observed in the ENACS the completeness of the redshift determinations does not depend on distance from the cluster center. This conclusion is strengthened by a comparison of our spectroscopic catalogue with the nominally complete photometric catalogues of Dressler (1980b), for the 10 clusters that we have in common. Again, we detect no dependence of the completeness on clustercentric distance.

We conclude therefore that the magnitude bias, which causes the apparent fraction of ELG to increase strongly towards the magnitude limit of the ENACS, only affects the estimation of the intrinsic ELG fraction. As is apparent from Fig. 1, that bias can be avoided by restricting the analysis to the 585 ELG for which also an absorption-line redshift could be obtained. However, it must be realized that this remedy against the magnitude bias for ELG has one disadvantage: it is likely to select against late-type spirals as these occur preferentially in the class of ELG without absorption-line redshift. We will come back to this in Sect. 3.2.

For surveys of (cluster) galaxies at higher redshifts (and fainter apparent magnitudes), which therefore have an inevitable observational bias against galaxies without detectable emission lines, this bias can in general *not* be corrected. Unless one has redshifts for all galaxies, e.g. down to a given magnitude limit, conclusions drawn from such 'incomplete' samples can be seriously biased, as they refer mostly to ELG. One obvious example is the determination of the fraction of ELG as a function of redshift, but e.g. also the determination of the evolution of cluster properties can be seriously affected. This problem may be aggravated if, as we will discuss below (see Sect. 5), the spatial distributions of ELG and non-ELG are not the same.

3. The ELG fraction in clusters and the field

3.1. Bias against galaxies without emission lines

In Fig. 2 we show the fraction of ELG as a function of apparent magnitude. The open symbols represent the *apparent* ELG fraction, calculated as the total number of galaxies in the ENACS with emission lines, divided by the total number of galaxies in the ENACS in the same magnitude range, viz. as:

$$f_{ELG} = \frac{\sum_{i=1}^{n} N_{ELG,i}}{\sum_{i=1}^{n} N_i} \quad (1)$$

where n is the number of systems, each containing $N_i \geq 10$ galaxies with redshifts, of which $N_{ELG,i}$ are ELG. The strong increase of the apparent ELG fraction towards fainter magnitudes is evident. As discussed in Sect. 2.5, this increase must be

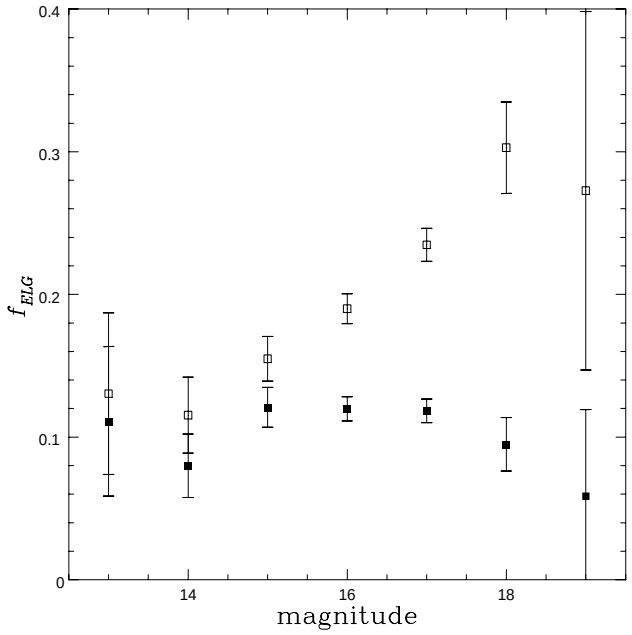

Fig. 2. The *apparent* fraction of ELG (open squares), determined using all galaxies, and the *true* fraction of ELG (filled squares) determined as the fraction of galaxies that have absorption- *and* emission-line redshifts among all galaxies with absorption-line redshifts, as a function of magnitude (R_{25}). Poissonian error bars are shown.

due to the bias that operates against the successful determination of redshifts for faint galaxies without emission lines.

This bias can be overcome if we calculate the fraction of ELG as the ratio of the number of the ELG for which also an absorption-line redshift is available, by the total number of galaxies with an absorption-line redshift. By definition, the magnitude bias does not operate in this comparison. The filled symbols in Fig. 2 give the resulting ELG fraction as a function of magnitude. As we anticipated, there is essentially no dependence of this corrected, *true* ELG fraction on magnitude, and it is considerably lower than the apparent fraction, especially at fainter magnitudes. Only for the brighter galaxies, for which there is no bias against the detection of an absorption-line based redshift, are the apparent and true ELG fraction essentially identical.

The apparent ELG fraction in the ENACS is 0.21 (= 1169 / 5634), but the corrected value is 0.12 (= 586 / 5051). In this paper we will always distinguish between the apparent and true ELG fractions, where the latter is calculated from the sample of all galaxies with absorption-line redshifts.

As far as we are aware, the correction for magnitude bias has not been applied in earlier work on the ELG fraction. In comparing our results with other determinations this should always be kept in mind. It is quite possible that some of the earlier results are not affected by magnitude bias, but it is often difficult to find out if that is a reasonable assumption. In a comparison with the results of the ESO Slice Project (ESP, see e.g. Zucca et al. 1995), for which the same instrumentation was used as for the ENACS, there may be differences in bias which influence the result. The reason for this is that the fraction of galaxies with emission lines is larger in the field (the object of study in the ESP) than it is in our clusters.

All ELG fractions based on the ENACS include a small contribution from AGN. Among interlopers and in systems with $N \leq 3$ (which in the ENACS provide the best approximation to the 'field'), the AGN fraction is 0.022 ± 0.006. For the systems with $N \geq 20$ (real, massive clusters) it is only 0.007 ± 0.001. These values are lower than the values previously obtained by Dressler et al. (1985), Hill & Oegerle (1993), and Salzer et al. (1989, 1995), but this may be due (at least partly) to the fact that we have been conservative in classifying galaxies as AGN, and have probably accepted only those with the strongest and broadest lines (see Sect. 2.4). The ratio of the AGN fraction in the field and in clusters is 3 ± 1, consistent with the value we find for all ELG (see Sect. 3.2). Dressler et al. (1985) found a similar value for the ratio between the AGN fraction in the field and in clusters.

3.2. The fraction of ELG in clusters and in the field

The ELG fractions in clusters and field have been studied by several authors, in order to find out if there is evidence for a difference in the occurence of ELG which can be traced to the influence of the environment in which galaxies live. Even though the ENACS, by its very nature, does not contain many field galaxies, it contains a sufficient number that we can investigate possible differences between the ELG fractions in the field and in clusters.

It is not trivial to identify the field galaxies in the ENACS. The main reason is that galaxies that are in small groups with only a few measured redshifts could, on the one hand, be in the field but, on the other hand, they could equally well be 'tips of the iceberg'. In other words: the number of *measured* redshifts in a group is not a good criterion for assigning galaxies to the field or to a cluster. One thing that is fairly certain is that the interlopers that were removed from the systems on the basis of their position *and* velocity (see Sect. 2.2) belong to the field and we consider them to be the best approximation to the field in the ENACS. Second best are the isolated galaxies. Finally, galaxies in groups with at most 3 measured redshifts are acceptable candidates for field galaxies, since the reality of such groups with less than 4 members is doubtful, as the definition of systems with such a small number of members is not at all robust (see Paper I). To a lesser extent the systems with 4 to about 10 redshifts also do not have a very robust definition (ibid.) but those we have included neither as cluster nor as field in the comparison between field and clusters. Finally, systems with at least 10 measured redshifts are very likely to be real clusters or groups.

In Table 2 we show the resulting ELG fractions for the three classes of environment. Note that for all three categories the fractions have been calculated as in Sect. 3.1. For each class we have calculated the apparent as well as the true ELG fractions. The ELG fractions for the interlopers and the $N \leq 3$ systems are quite similar, and they are both quite different from the average ELG fraction in clusters. Because the galaxies for

Table 2. The fraction of ELG in different environments

Environment	f_{ELG}	
	apparent	true
Interlopers	0.35 ± 0.08	0.22 ± 0.07
Systems with $N \leq 3$	0.43 ± 0.03	0.21 ± 0.02
Systems with $N \geq 10$	0.16 ± 0.01	0.10 ± 0.01

which the redshift is based solely on emission lines have, on average, fainter magnitudes, the difference appears most striking in the apparent fractions, but it is equally significant in the bias-corrected, true values.

From the numbers in Table 2 we conclude that it is not unreasonable to assume that the interlopers and the galaxies in the $N \leq 3$ systems give a fair estimate of the ELG fraction in the field: combining the two classes we obtain apparent and true ELG fractions of 0.42 ± 0.03 and 0.21 ± 0.02 respectively. It is interesting to note that the corresponding numbers for the systems with $4 \leq N \leq 9$ are 0.30 ± 0.03 and 0.15 ± 0.02. This clearly suggests that these systems are indeed intermediate between real clusters and field galaxies. Additional support for the assumption that the systems with $N \geq 10$ are indeed almost all clusters is provided by the ELG fractions for the systems with $N \geq 20$. For those, there is no doubt at all that they are clusters and their average apparent and corrected ELG fractions are 0.15 ± 0.01 and 0.10 ± 0.01 respectively.

Our *apparent* ELG fraction for the 'field' is quite similar to that derived by Zucca et al. (1995), who found a value of ~ 0.5 in the ESO Slice Project. This is quite gratifying, as these authors obtained their spectra using an observational set-up that was essentially identical to ours. It is true that the average redshift in their survey is about a factor of 2 larger than in the ENACS, and their result therefore applies to a larger region in the centre of the galaxies than does ours. Apparently, this has little or no effect on the apparent ELG fraction. The ELG fraction found by Salzer et al. (1995) is 0.31, i.e. intermediate between our *apparent* and *true* fractions.

Our apparent ELG fraction for the field is significantly lower than the value of 0.75 ± 0.05 that was found by Gisler (1978). On the contrary, it is higher than the value of 0.31 ± 0.05 found by Dressler et al. (1985), as well as the value of 0.27 ± 0.08 found by Hill & Oegerle (1993). However, as it is not clear whether we should compare the literature values with our apparent or bias-corrected values, the latter two determinations could actually be consistent with our result.

A similar uncertainty is present in the comparison of our cluster ELG fraction with earlier estimates in the literature. Our apparent value of 0.16 ± 0.01 is consistent with the value found by Gisler (1978) in compact clusters (0.17 ± 0.06), but quite a bit higher than the values of 0.07 ± 0.01 and 0.06 ± 0.01 found by Dressler et al. (1985), and Hill & Oegerle (1993), respectively. If the latter two literature values should in fact be compared with our bias-corrected value of 0.10 ± 0.01 the agreement becomes somewhat better, although not perfect. As we shall see in Sect. 3.3, part of the remaining difference in the cluster ELG fraction may be due to the composition of the cluster samples with respect to mass (or global velocity dispersion).

There are several other factors of this kind which can, at least in principle, influence the observed ELG fraction. Among these are: the average luminosity of the galaxy sample, the criterion by which cluster members and field galaxies are identified, and (as mentioned earlier) the linear sizes of the average aperture used in the spectroscopy. The latter factor may well explain the differences with the values obtained by Gisler (1978), who used spectra with a larger effective aperture; this may be the reason for the systematically high values that he obtained for the ELG fraction. On the other hand, the sample studied by Dressler et al. (1985) could be biased against late-type spirals and irregulars (see Dressler & Shectman 1988). As these have a relatively high ELG fraction, this might well explain why their ELG fractions (for cluster *as well as* for the field) are low.

Although the *absolute* values of the ELG fractions obtained by different authors may thus be difficult to compare (e.g. due to differences in observational set-up etc.), the *relative* fractions of ELG located in different environments might well be less dependent on such details. In the ENACS the ratio between the ELG fraction in the field and in clusters is 2.6 ± 0.3 (apparent) and 2.1 ± 0.3 (bias-corrected). The average ratios found previously are: 4.4 ± 1.7 (Gisler 1978), 4.4 ± 1.0 (Dressler et al. 1985) and 4.5 ± 1.4 (Hill & Oegerle 1993). The uncertainties are rather large, but there may be some evidence that details of the various techniques and the galaxy and/or cluster selection, have influenced even the *relative* frequency of occurence of ELG in cluster and field. On the other hand, the mix of the various types of galaxy may not be the same in the different samples so that, with different ELG fractions for the various galaxy types, the ratio between the ELG fractions are expected to be different.

In Table 3 we show the values of the ELG fraction for galaxies in clusters as a function of morphological type. These fractions are based on the ENACS data in combination with the morphologies determined by Dressler (1980b) for the 545 galaxies in the 10 clusters that are common between the ENACS and the Dressler catalogue. Almost all of these (namely 537) have an absorption-line ENACS redshift; 68 of the 537 galaxies (i.e. 13%) also have emission lines. Of the 68 ELG (none of which is an AGN), 60 are spirals or irregulars, 7 are S0s and 1 is an elliptical. We thus find that the fraction of ELG depends strongly on morphological type. Note that the ELG fractions in Table 3 are unbiased, as all galaxies used in the statistics have absorption-line redshifts.

It is also of interest to determine the fraction of spirals that we have detected as ELG. Of the 180 spirals in the sample of 537 galaxies, only 60 are ELG. So, while most of our ELG are late-type galaxies, the ELG represent only about $1/3$ of the total spiral population in our clusters.

Since the mix of galaxy types is a strong function of the density of the environment, one may ask whether the difference between the ELG fractions in the clusters and in the field can

Table 3. The fraction of ELG for cluster galaxies of different morphological types

Morphological type	f_{ELG}
E	0.01 ± 0.01
S0	0.03 ± 0.01
Sa, Sb	0.27 ± 0.05
Sc, Sd, I	0.40 ± 0.15
Unqualified S	0.28 ± 0.07

be totally attributed to a lower fraction of late-type galaxies in clusters. Following Dressler et al. (1985), we have used the ELG fractions of cluster galaxies for the different galaxy types, and convolved that with the distribution over galaxy type of field galaxies. This should yield the ELG fraction that clusters would have if their morphological mix were the same as that of the field. In the ENACS there are only very few field galaxies with known type. Therefore, we have assumed the field type mix given by Oemler (1974), with which we calculate an expected field ELG fraction of 0.23 ± 0.03. This value, which is based on the assumption that the dependence of ELG fraction over morphological type is identical in cluster and field, is of course fully consistent with our observed, bias-corrected value for the field ELG fraction.

This result is at variance with all previous findings on this point (Osterbrock 1960, Gisler 1978, Dressler et al. 1985, Hill & Oegerle 1993). It can be rephrased by saying that environmental effects probably do not affect the fraction of ELG, or the emission-line activity. Note that, had we not accounted for the magnitude bias (the fact that the apparent ELG fraction increases towards faint magnitudes), we would have come to the same conclusion as the above-mentioned authors. However, the magnitude bias is stronger for the field galaxies than for the cluster sample (because our field galaxies are on average fainter than our cluster galaxies). As a result, the need for different emission-line characteristics of field and cluster galaxies disappears if the bias is taken into account.

At this point we must come back to the selection against late-type spirals which is inherent in our calculation of the true ELG fraction, since the latter is based only on the ELG *with* absorption-line redshift (see Sect. 2.5). We have attempted to take this factor into account, by assuming that most of the ELG *without* absorption-line redshift in the field are late-type spirals. Our best estimate of the fraction of late-type spirals among our field spirals is about 50%, although we cannot exclude that it is 70%. Using the former fraction together with the ELG fractions for early- and late-type spirals in Table 3, we estimate an expected ELG fraction in the field of 0.26 ± 0.05 instead of 0.23 ± 0.03. This is still consistent with the observed true ELG fraction in the field of 0.21 ± 0.02, so that the conclusion in the preceding paragraph is not likely to be the result of the selection against late-type spirals in the calculation of true ELG fractions.

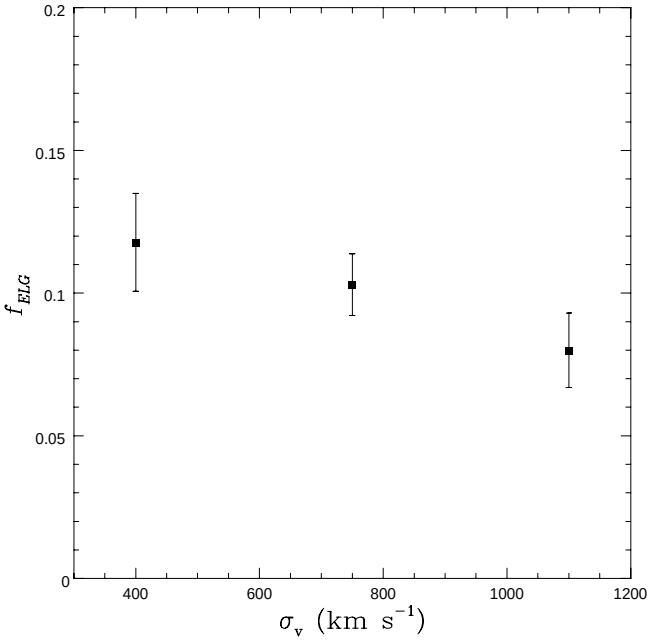

Fig. 3. The fraction of ELG in systems with different velocity dispersions, σ_V . Poissonian error bars are shown.

3.3. The ELG fraction as a function of velocity dispersion

In Sect. 3.2 we found that f_{ELG} is practically independent of N for systems with $N \geq 10$. On the other hand, we also noted that some of the differences between our ELG fractions and those of other authors might be due to different composition of cluster samples in terms of mass, or some other physically relevant parameter. An obvious question is therefore if, within the ENACS data, we observe a dependence of the ELG fraction on the global velocity dispersion of the system. In Fig. 3 we show f_{ELG} as a function of velocity dispersion, where f_{ELG} was calculated as in Sect. 3.1 in three separate intervals of σ_V . For this figure, we have used only the 75 systems with $N \geq 20$ of sample 3, as these are very likely to be bona-fide rich clusters. It is clear that there is a significant decrease of the ELG fraction with increasing velocity dispersion, by a factor of 1.5 over the range of dispersions sampled. Within the errors, the same result is obtained if we use the sample of all 120 systems with $N \geq 10$ listed in Table 1.

On average, clusters with smaller velocity dispersions are less rich than clusters with larger velocity dispersions (see, e.g., Paper II). Since essentially all ELG are spirals, the above result is thus consistent with van den Bergh's (1962) finding that the fraction of late-type galaxies is higher in poorer clusters. We must point out that the f_{ELG} dependence on σ_V is not induced by different sizes of the area over which we obtained spectroscopy for the different clusters. This could have an effect, in principle, as a consequence of the morphology-density relation and because the clusters for which the observations covered a larger area have a (slightly) higher σ_V than average. However, if we consider only galaxies within 1 h^{-1} Mpc of their respective

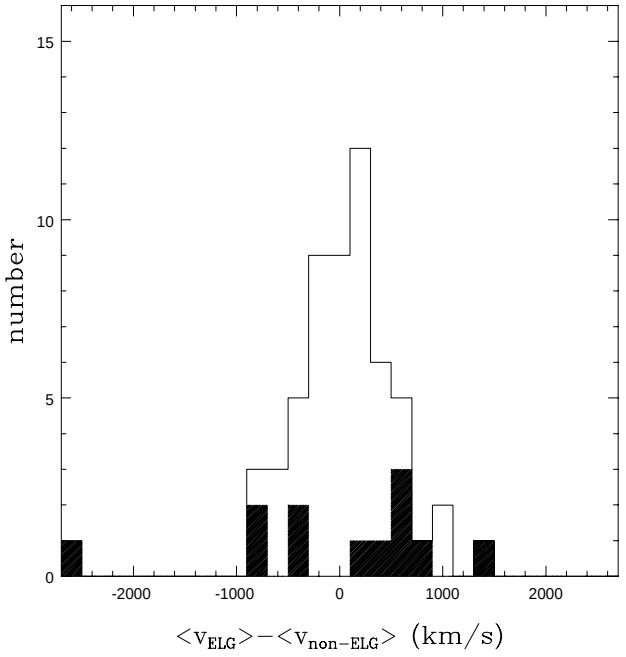

Fig. 4. The distribution of $<v>_{ELG} - <v>_{non-ELG}$ for the 57 clusters with at least 5 ELG within $\pm 3\sigma$ from the mean velocity. The twelve clusters for which this difference is significant at more than 2σ have been indicated.

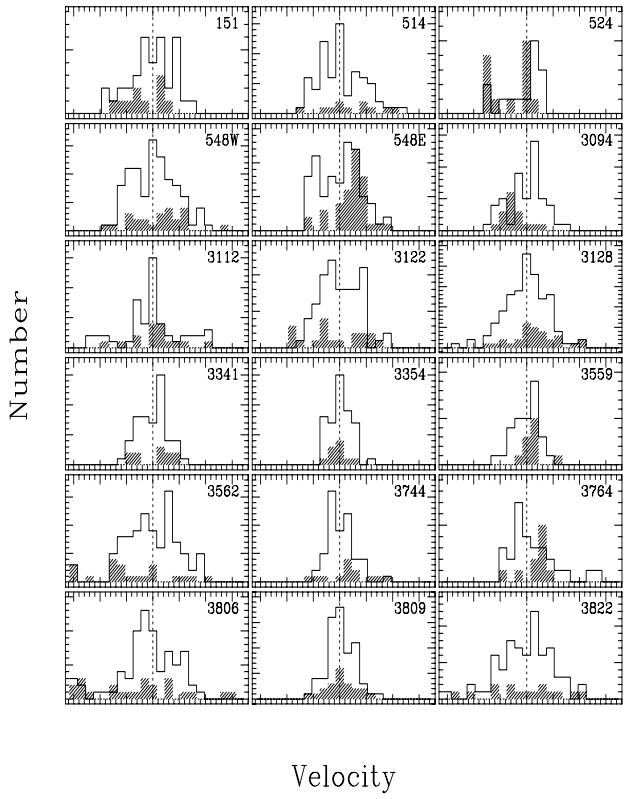

Fig. 5. Velocity Distributions of non-ELG and ELG (hatched histogram) in the 18 clusters with at least 10 ELG. The dashed line in each panel indicates the average velocity of the system. One division on the horizontal (velocity-) scale corresponds to 200 km s^{-1} and the binwidth is 250 km s^{-1} . One division on the vertical scale corresponds to one galaxy.

cluster center, in those 51 clusters (with $N \geq 20$) observed at least out to 1 h^{-1} Mpc , the relation between f_{ELG} and σ_V is unchanged.

We conclude therefore that there is a significant decrease of the fraction of ELG, with increasing σ_V , which must reflect a dependence on mass.

4. The global kinematics of ELG and non-ELG

In this section we analyze the global kinematics of ELG and non-ELG. Before we enter into the details of this discussion we want to emphasize the following important point. All the results that we will obtain in this section, either on differences between ELG and non-ELG in average velocity or in velocity dispersion, are based on the implicit assumption that both types of galaxies consist of single systems. In other words: we have calculated a single average velocity (or velocity dispersion) for both ELG and non-ELG. If this assumption is incorrect (e.g. because the ELG do not have a smooth spatial distribution, but instead are in several compact groups within a cluster) the interpretation of the results obviously becomes more complicated. We will return to this question in Sect. 6.

4.1. Average velocities

Zabludoff & Franx (1993) noted that the average velocity of late-type galaxies was different from that of early-type galaxies in 3 of the 6 clusters they examined. They interpreted this as evidence for anisotropic infall of groups of spirals into the cluster. However, since their analysis is limited to 6 clusters, one cannot draw general conclusions from this result.

Here, we address the same issue on the basis of our sample of 57 clusters in which at least 5 ELG were found (sample 1). For these systems, we determined the average velocities of both ELG and non-ELG, as well as the associated 1σ errors, which were calculated with the jack-knife technique (see, e.g., Beers et al. 1990). For the 12 clusters in which the velocity difference between ELG and non-ELG exceeds 2σ, we give details in Table 4. The distribution of the differences $<v>_{ELG} - <v>_{non-ELG}$ in the 57 systems is shown in Fig. 4.

We thus find a much lower fraction of clusters with significant differences in the average velocities of ELG and non-ELG than did Zabludoff & Franx. One might think that the two results could be consistent, if in many of our clusters there would be a real difference which has been masked by the effects of limited statistics. However, in Sect. 4.2 we will show, from the distributions of velocity difference between galaxy pairs, that this is unlikely to be the case. In addition, the same low fraction of significant velocity offsets is found among the 20 systems that contain at least 10 ELG.

Table 4. The average velocity differences between ELG and non-ELG in those clusters where the difference is larger than 2σ

Abell nr	$<v>_{non-ELG}$ km s^{-1}			ΔV km s^{-1}			N, N_{ELG}	
151	12122	±	112	-340	±	161	25	5
151	29537	±	165	367	±	175	35	5
548E	12268	±	99	530	±	153	114	38
548	25186	±	459	1496	±	588	14	8
548	30081	±	122	575	±	220	21	6
2819	22239	±	74	243	±	106	49	6
2819	25889	±	52	-712	±	313	43	6
3094	20155	±	124	-489	±	163	66	16
3151	20414	±	143	-2555	±	583	38	6
3562	14744	±	123	-862	±	382	116	21
3693	26887	±	213	791	±	268	16	5
3764	22329	±	206	555	±	231	38	10

For each of the 18 systems with at least 10 ELG (sample 2), we show in Fig. 5 the velocity distributions of ELG and non-ELG separately. Note that this figure does not include every system listed in Table 4, because quite a few of those have less than 10 ELG. For the 4 systems in the figure that also appear in Table 4 (A548E, A3094, A3562 and A3764) the histograms clearly give a visual confirmation of the existence of a velocity difference. There are several systems with intrigueingly uneven velocity distributions for, in particular the ELG, but with the present statistics it is impossible to say if those are indeed clusters with real velocity differences between ELG and non-ELG.

4.2. Velocity dispersions

For the systems with significant velocity differences between ELG and non-ELG that are shown in Fig. 5, the numerical evidence is supported visually by the figure. However, it is impossible to say from that figure if there exist significant differences between the *velocity dispersions* of ELG and non-ELG. It turns out, however, that among the 18 systems with at least 10 ELG, 3 have a $\sigma_{\rm V}$ difference between ELG and non-ELG that is significant at a level of more than 2 σ. The values of $\sigma_{{\rm V},non-ELG}$ and ($\sigma_{{\rm V},ELG}$ - $\sigma_{{\rm V},non-ELG}$) for these systems and their jack-knife errors are given in cols.(2) and (3) of Table 5. It is interesting that all 3 differences are positive, i.e. that in all 3 cases the $\sigma_{\rm V}$ of the ELG is larger than that of the non-ELG.

We have followed up this conclusion by considering all 75 systems of sample 3 with $N \geq 20$. For 57 of these, it is not possible to derive a meaningful $\sigma_{\rm V}$ estimate for the ELG separately. However, for 71 of the 75 systems (4 of which do not have an ELG), one can compare the $\sigma_{\rm V}$ values derived for the total galaxy population with those for the non-ELG only (i.e. excluding the ELG). As non-ELG are the dominant population, we expect that the change in $\sigma_{\rm V}$ on excluding the ELG will be quite small, but combining the results for all 71 systems may nevertheless give a significant result.

Table 5. Significant velocity-dispersion differences between ELG and non-ELG

Abell nr	$\sigma_{{\rm V},non-ELG}$ km s^{-1}			$\Delta\sigma_{\rm V}$ km s^{-1}			N, N_{ELG}	
3122	706	±	59	354	±	119	89	18
3744	474	±	55	519	±	80	66	13
3806	953	±	113	763	±	275	97	23

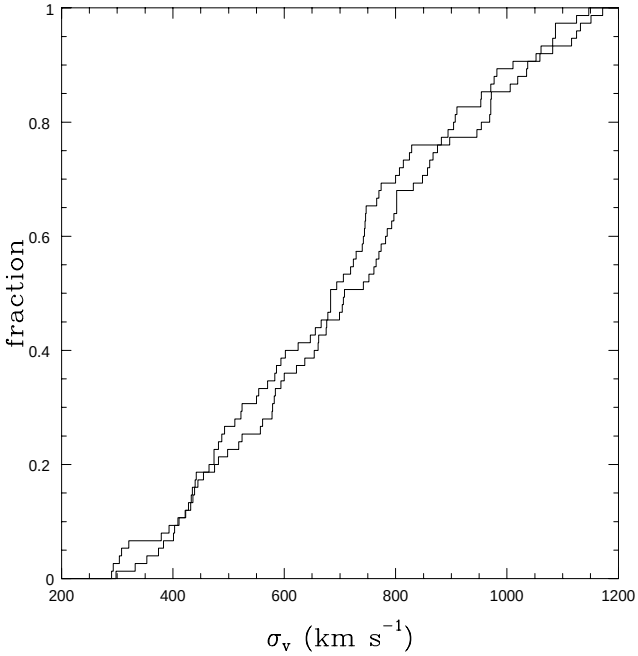

Fig. 6. The cumulative $\sigma_{\rm V}$ distributions for non-ELG only (thin line), and for all the galaxies (ELG+non-ELG, thick line) in the 75 clusters with at least 20 members.

In Fig. 6 we show the two cumulative $\sigma_{\rm V}$ -distributions for all the galaxies (ELG+non-ELG) and for non-ELG only, in the 75 clusters with at least 20 members (i.e. the 4 clusters without ELG are included in the Figure). The removal of the ELG from the cluster samples in general lowers the value of $\sigma_{\rm V}$; a Wilcoxon test (see e.g. Press et al. 1986) indicates that the ELG+non-ELG $\sigma_{\rm V}$ distribution is different from that of the non-ELG at the > 0.999 conf.level, and that $\sigma_{\rm V}$ of ELG+non-ELG is, on average, larger than $\sigma_{\rm V}$ of the non-ELG.

4.3. Velocity distributions

In order to examine the kinematical properties of ELG and non-ELG further, we have put together all galaxies in the 75 clusters in sample 3 in a single, 'synthetic', cluster. We define a "normalized velocity difference", Δv_n , with respect to the average velocity of the system to which the galaxy belongs, which is

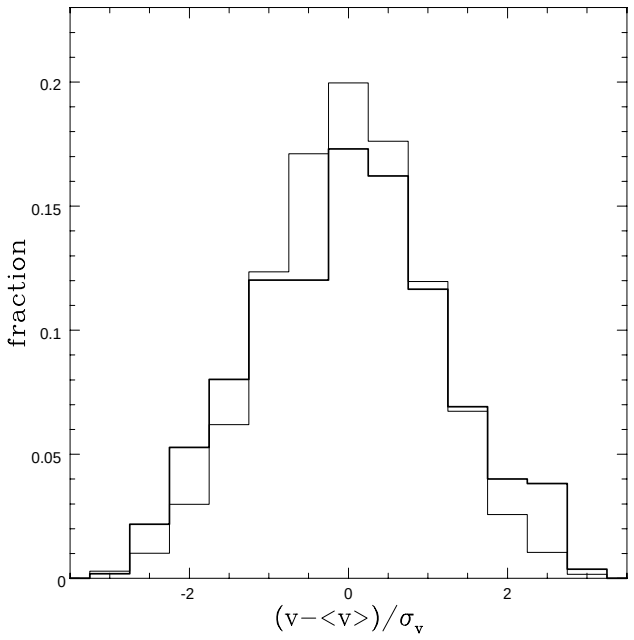

Fig. 7. The normalized-velocity histograms for the total sample of 549 ELG (thick line) and 3150 non-ELG (thin line) in the 75 clusters with at least 20 members.

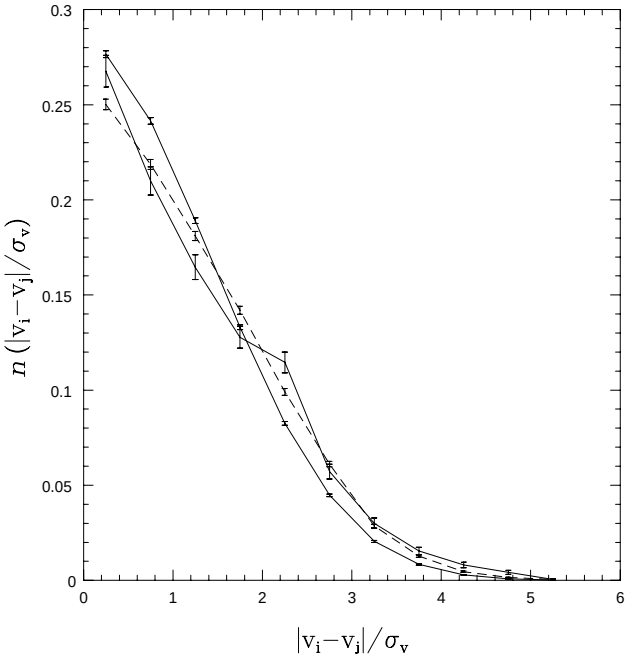

Fig. 8. The distribution of velocity differences among pairs of non-ELG (thin line), pairs of ELG (thick line), and mixed pairs of one non-ELG and one ELG (dashed line), normalized to the velocity dispersion of the system to which the pair belongs. Poissonian error-bars are shown.

normalized with respect to the velocity dispersion of the parent system, viz. $\Delta v_n = (v - < v >)/\sigma_v$.

For this discussion we could have included the systems with $10 \leq N < 20$, but we have not done so, because later on we will include positional information which requires the centre to be known with sufficient accuracy. When comparing the Δv_n -distributions of ELG and non-ELG, we do not want to be strongly affected by the tails of these distributions. As our interloper rejection method was only applied to clusters with more than 50 galaxies (see Sect. 2.2), it is possible that a few outliers are still present in the systems with less than 50 galaxies. For the preceding analysis, in which we used robust estimators, such outliers were not very important. However, combining data for many systems for which the average velocity is not known exactly will produce longer tails in the velocity distribution. As for some of the following analyses we cannot use robust estimators we have to get rid of possible outliers. To that end we have applied a 3σ-clipping criterion (Yahil & Vidal 1977). This removes 30 galaxies in total (among which are 9 ELG) and yields a 'synthetic' cluster with 3699 galaxies, among which are 549 ELG.

The ELG and non-ELG Δv_n -distributions are shown in Fig. 7. The Δv_n -distribution for ELG is broader than that for non-ELG; the KS-test gives a probability of 0.029 that the two distributions are drawn from the same parent population. The dispersion of the Δv_n 's of the ELG is 21 ± 2 % larger than the dispersion of the Δv_n 's of the non-ELG.

Among the 549 ELG, 37 are AGN; the KS-test indicates that the Δv_n -distributions of AGN and non-ELG are significantly different (with a probability of 0.047 for the two distributions to be drawn from the same parent population), but the Δv_n -distributions of AGN and the other 512 ELG are not. Therefore, AGN seem to follow the velocity distribution of the other ELG.

In principle there are two possible explanations for the wider Δv_n distribution for the ELG. On the one hand, the ratio of $\sigma_{v,ELG}$ and $\sigma_{v,non-ELG}$ may be *larger than unity* by roughly the same amount in *essentially all* systems. On the other hand, the broader distribution of the Δv_n of the ELG could be due to the fact that we have superposed many ELG systems. Even if, in most systems, the σ_v of the ELG were identical to the σ_v of the non-ELG, the width of the Δv_n distribution could be larger for ELG than for non-ELG if the *average velocities* of ELG and non-ELG are *substantially different* in the large majority of the systems. The reason is that the Δv_n 's are calculated with the overall values of $< v >$ and σ_V, which are determined primarily by the non-ELG.

These two possible explanations are obviously extreme cases, and it is very unlikely that one of them applies exclusively. In Sect. 4.1 we saw that in a small fraction of the clusters there is evidence for a significant offset between the average velocities of ELG and non-ELG. However, we could not tell whether such offsets occur in essentially all systems (but were not detectable in many systems due to limited statistics). Here, we will show that the main reason for the apparently larger σ_v of the ELG must be that the intrinsic σ_v of the ELG is about 20% larger than that of the non-ELG. In other words: only a small part of the larger dispersion of the ELG is due to the fact that we have combined several narrower gaussians with different

means. This conclusion is based on an analysis of the pairwise velocity differences of the ELG.

In Fig. 8 we show the sum (over all systems) of the distribution, for all galaxy pairs in a given system, of the absolute value of the pairwise velocity difference (again, normalized to the velocity dispersion of the system to which the two galaxies belong), i.e. $\mid v_i - v_j \mid /\sigma_{\rm v}$. These distributions were calculated separately for pairs of non-ELG (thin line), pairs of ELG (thick line), and for mixed pairs of an ELG and a non-ELG (dashed line). The three distributions have been normalized to the total number of pairs of each kind; clearly the uncertainties are largest for the ELG/ELG-pairs. If essentially all ratios $\sigma_{{\rm v},ELG}$ / $\sigma_{{\rm v},non-ELG}$ for the individual systems would be larger than one (and if velocity offsets between ELG and non-ELG were non-existent) one would expect three gaussian distributions in Fig. 8, with widths increasing from the non-ELG/non-ELG, via the non-ELG/ELG to the ELG/ELG pairs.

The distributions for the non-ELG/non-ELG and non-ELG/ELG pairs are indeed very close to gaussian, and the non-ELG/ELG distribution is broader than that of the non-ELG/non-ELG pairs. However, the distribution for the ELG/ELG pairs is quite different from this gaussian expectation. The ELG/ELG distribution for Δv smaller than $\approx$ 2 has a curvature opposite to that of a gaussian. Therefore, there must be a component that produces an n($\mid v_i - v_j \mid /\sigma_{\rm v}$) that is small for small values of $\mid v_i - v_j \mid /\sigma_{\rm v}$ and has a peak at $\mid v_i - v_j \mid /\sigma_{\rm v}$ of about 2 and then decreases again. One way to produce such a component is by having systems in which the ELG have a velocity offset of about one $\sigma_{\rm v}$ with regard to the non-ELG. However, at the same time, there must be a second component which produces the broadening of the ELG/ELG distribution for large values of $\mid v_i - v_j \mid /\sigma_{\rm v}$ (say, larger than about 2). In other words: we are led to a schematic model with two components in the ELG velocity distribution, one with fairly small internal $\sigma_{\rm v}$ and significant velocity offsets, and another with a global $\sigma_{\rm v}$ that is larger than the $\sigma_{\rm v}$ of the non-ELG but without a significant velocity offset.

We have attempted to estimate the relative importance of these two components by some simple modeling. Although there is not a single, unique solution, it appears that the distribution for the ELG/ELG pairs in Fig. 8 requires that $\sim$25% of the ELG reside in systems with an average velocity offset of about 600 km s^{-1} (i.e. almost equal to the value of the global σ_V). However, the internal $\sigma_{\rm v}$ of these ELG systems with significant velocity offsets must be small, i.e. less than about half the value of $\sigma_{{\rm v},non-ELG}$. If the fraction of ELG in these systems is much larger or smaller than 25% and/or the $\sigma_{\rm v}$ values of these systems is comparable to the $\sigma_{\rm v}$ values of the non-ELG, the steep slope of the ELG/ELG distribution at small $\mid v_i - v_j \mid /\sigma_{\rm v}$ values (say, below 1.5) cannot be reproduced.

For the other $\sim$75% of ELG, i.e. those in the systems without large velocity offsets, the global value of $\sigma_{\rm v}$ must be a factor of about 1.25 larger than $\sigma_{{\rm v},non-ELG}$ in order to reproduce the number of ELG/ELG pairs for values of $\mid v_i - v_j \mid /\sigma_{\rm v}$ between 2 and 4 to 5. This simple model clearly cannot give information on how the latter 75% of ELG are distributed, and how their $\sigma_{{\rm v},ELG}$ (of, on average, 1.25 $\sigma_{{\rm v},non-ELG}$) comes about. As mentioned earlier, they can either be essentially isolated galaxies (and distributed more or less uniformly in their parent clusters), or they may be in compact groups, or a combination of these. From Fig. 5 one gets the impression that both cases occur. We will return to this question in Sect. 6.

It is worth remembering that in Sect. 4.1 we found that for 12 out of 57 systems there is a significant difference in the average velocities of ELG and non-ELG. The observed offsets range from about 300 to 1400 km s^{-1} (with a median of about 600 km s^{-1}). Both the fraction of systems with a significant offset and the size of the offsets that we derived here from a simple model thus agree very nicely with the observed values.

Finally, we note that the distribution of normalized velocities for the AGN subset of the ELG cannot be distinguished from that of the non-ELG or ELG, due to the limited number of AGN in the ENACS.

5. The spatial distributions of ELG and non-ELG

We have analyzed the spatial distributions of ELG and non-ELG (and possible differences between them) in several different ways. First, we have used the harmonic mean pair distances, $\rm r_h$, for which no cluster centre needs to be known. As the number of ELG per system is often not very large, the determination of $\rm r_h$ for the ELG separately is mostly not very robust. We have therefore compared the cumulative $\rm r_h$ distributions of all cluster galaxies (ELG+non-ELG) and of non-ELG only, for the 75 systems of sample 3. According to the Wilcoxon test, the two distributions are significantly different (at the $>$ .999 conf.level). More specifically: when ELG are excluded from the systems, smaller $\rm r_h$ values are found. Although these differences are systematic, they are quite small because the average fraction of ELG is only 16 %. The average reduction of $\rm r_h$ is only 3 % which implies that $\rm r_{h},_{ELG}$ is larger than $\rm r_{h},_{non-ELG}$ by $\sim$ 20 %.

Another way to look at the differences in the spatial distribution of ELG and non-ELG is to study the local densities of their immediate environment. We calculated the local density, Σ, as the surface density of galaxies within a circular area centered on the galaxy, with radius equal to the distance to its $\rm N^{1/2}$-th neighbour, where N is the total number of galaxies in the system. In Fig. 9 we show the normalized distributions of the values of Σ for ELG and non-ELG, for all galaxies in the 75 systems of sample 3. The distributions are significantly different (at the $>$ 0.999 conf.level), and the local density around ELG is, on average, 0.72 ± 0.03 times the density around non-ELG.

Both tests show that the spatial distribution of the ELG is significantly broader than that of the non-ELG. Additional information on the differences between the spatial distributions of ELG and non-ELG can be obtained from a comparison of the density profiles of the two classes. Because the number of ELG in a cluster is rather small, a reliable density profile of the ELG can only be obtained from the combination of all systems. We then assume implicitly that different clusters have similar profiles. This is not unreasonable, since cluster density profiles have similar slopes (see, e.g., Lubin & Bahcall 1993, Girardi

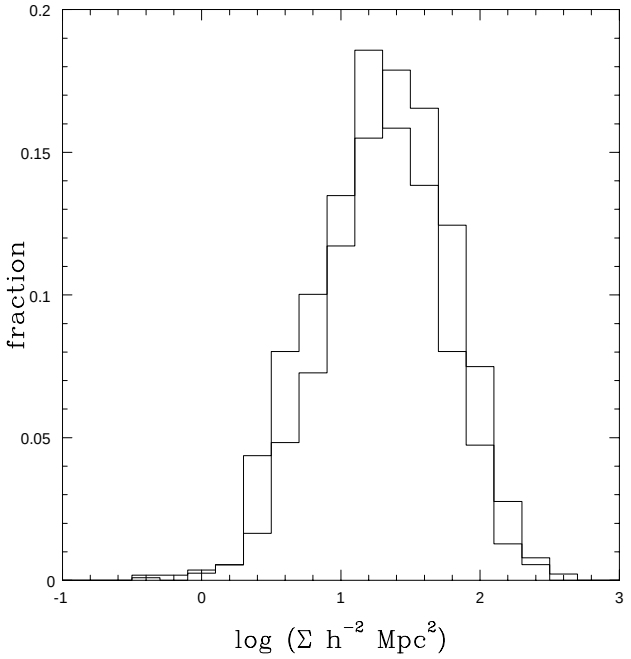

Fig. 9. The distribution of the logarithm of the local surface densities, Σ, for ELG (thick line) and non-ELG (thin line) in 75 clusters with $N \geq 20$. See the text for the definition of local densities.

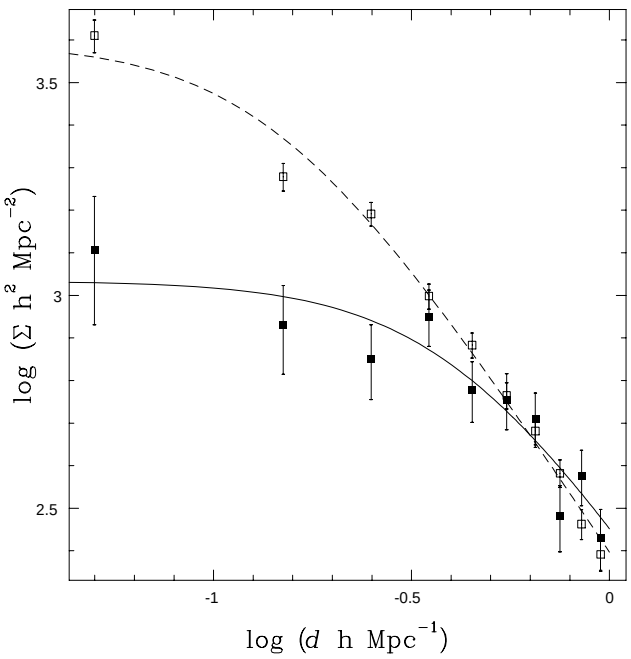

Fig. 10. The surface density profiles for ELG (filled symbols) and non-ELG (open symbols) for 51 clusters sampled at least out to 1 h^{-1} Mpc , and with at least 20 galaxy members. The continuous and dashed lines are the fits to the ELG and non-ELG distributions, respectively with $\beta = -0.71$. Note that the ELG profile has been moved up by +0.65 in $\log \Sigma$ for an easier comparison with the non-ELG profile.

et al. 1995), although their core-radii have a large spread (see, e.g., Sarazin 1986; Girardi et al. 1995; note, however, that the very existence of cluster cores is doubtful, see, e.g., Beers & Tonry 1986, Merritt & Gebhardt 1995). All these possible complications are not very important at this point, because here we are only interested in the relation between the density profiles of ELG and non-ELG.

In constructing the surface density profiles we have considered only the 51 systems from sample 3 for which the data extend at least out to 1 h^{-1} Mpc , in order to avoid possible problems of incompleteness, and we have limited our analysis to galaxies within 1 h^{-1} Mpc .

The density profiles of ELG and non-ELG are shown in Fig. 10, and they have been fitted by the usual β-model:

$$\Sigma(d) = \Sigma(0)[1 + (d/r_c)^2]^{-\beta} \quad (2)$$

The maximum-likelihood fit to the unbinned distribution of the non-ELG yields the following values: $\beta = -0.71 \pm 0.05$, $r_c = 0.15 \pm 0.04$ h^{-1} Mpc , with a reduced χ^2 of 1.9 (8 degrees of freedom). For the ELG we obtain maximum-likelihood values $\beta = -1.3 \pm 1.2$, $r_c = 0.8 \pm 0.8$ h^{-1} Mpc , with a reduced χ^2 of 0.9 (again, 8 degrees of freedom). The simultaneously fitted model-parameters for the ELG are quite uncertain, largely due to the flatness of the ELG density profile within 1 h^{-1} Mpc . We have therefore made a second fit to the ELG data in which we have taken $\beta = -0.71$ (equal to the value for the non-ELG), which gives $r_c = 0.42 \pm 0.07$ h^{-1} Mpc for the ELG.

The β-models with $\beta = -0.71$ are also shown in Fig. 10. The fit for the non-ELG is not very good because of the peak in the first bin (note that a peaky profile is expected when an accurate choice of the cluster center is made; see Beers & Tonry 1986). Nevertheless, the values found for r_c and β are consistent with recent results obtained by Lubin & Bahcall (1993) and Girardi et al. (1995).

We note in passing that the AGN, which are a subset of the ELG, have a spatial distribution that cannot be distinguished from that of the ELG; however, their distribution is different from that of the non-ELG.

6. Correlations between velocity and position

In Sect. 4 and Sect. 5 we discussed separately the kinematics and spatial distribution of ELG and non-ELG and the differences between them. From the discussion in Sect. 4.3 we concluded that there is evidence for two ELG populations, one with a σ_V that is considerably smaller than the overall value and with significant velocity offsets (with regard to the non-ELG), and another with σ_V larger than the overall value and without significant velocity offsets. This result immediately raises the question of possible correlations between velocity and position or, in other words: of structure in phase-space. Do the characters of the phase-space distributions of ELG and non-ELG differ and if so, in what way. What evidence do we have on substructure, i.e. on the existence of spatially and/or kinematically compact groups, and are there differences between ELG and non-ELG in that respect.

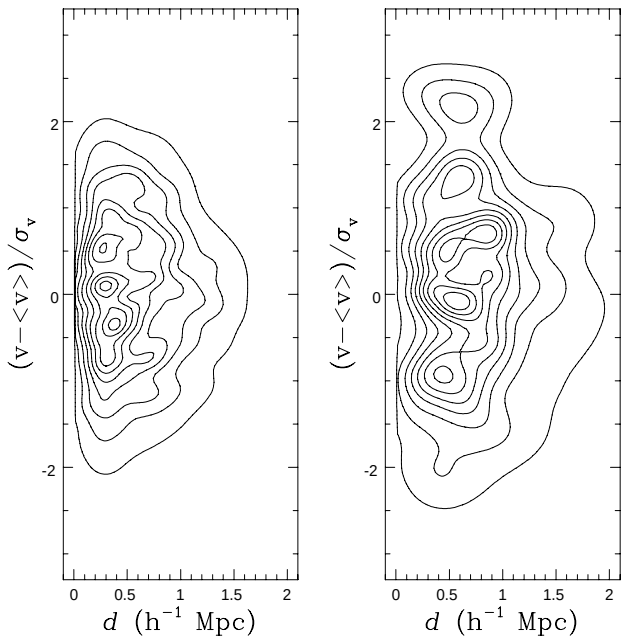

Fig. 11. Adaptive-kernel maps of the 2-dimensional distribution w.r.t normalized velocity and clustercentric distance for the non-ELG (left panel) and ELG (right panel) in the synthetic cluster constructed from the 75 systems with $N \geq 20$.

6.1. The phase-space distributions

In Fig. 11 we show adaptive kernel maps (see e.g. Merritt & Gebhardt 1995) of the distributions of both ELG and non-ELG with regard to normalized-velocity (see Sect. 4.3) and clustercentric distance, for the synthetic cluster constructed from the 75 systems with $N \geq 20$. Note that a velocity limit of $\pm 3\sigma_{\rm V}$ has been applied, as before. A 2 - D KS-test (Fasano & Franceschini 1987) gives a probability < 0.001 that the two distributions are drawn from the same parent distribution. This is hardly surprising in view of the fact that we found a less centrally concentrated spatial distribution for the ELG than for the non-ELG, as well as a $\sigma_{\rm V}$ that is $\sim 20\%$ larger for the (majority of the) ELG than it is for the non-ELG. Both effects are clearly visible in Fig. 11. However, it is very difficult to tell which features in the distributions in Fig. 11 represent real substructure, if only because the distributions represent sums over all 75 clusters. It is equally difficult to estimate from Fig. 11 what fraction of the galaxies is in real substructure that is compact both in position and velocity.

For a more quantitative discussion of this point we consider the distributions of $\Delta {\rm r}_{proj}$ and Δv_n for *pairs* of galaxies (rather than individual galaxies) and, in particular, pairs of **nearest** *neighbours from the same class*. For the non-ELG we use all 75 systems in sample 3 (with $N \geq 20$) which contain 3150 galaxies in total. The number of non-ELG nearest-neighbour pairs is 2219. This is less than the number of galaxies because when B is the nearest neighbour of A *and*, at the same time, A happens to be the nearest neighbour of B, the pair A-B is used only once. For the ELG we have considered only the 18 systems with ${\rm N}_{ELG} \geq 10$ (for reasons that will become apparent); these 18 systems contain 306 ELG (3 ELG were removed in the $\pm 3\sigma$ clipping) with which we have formed 207 nearest-neighbour pairs.

In Fig. 12 we show the normalized distributions of $\Delta {\rm r}_{proj}$ and Δv_n (i.e. $\Delta v/\sigma_{\rm V}$) for nearest neighbours, for non-ELG (upper two panels) and ELG (lower two panels). The global differences between the two sets of distributions are not unexpected: the lower surface density of ELG gives rise to larger $\Delta {\rm r}_{proj}$ for ELG-ELG pairs; similarly, the larger global $\sigma_{\rm V}$ of the ELG causes a wider Δv_n distribution for the ELG-ELG pairs. In order to get a more quantitative estimate of the amount of real, compact substructure in Fig. 11, we have compared these distributions with scrambled versions of the same. The scrambled data should give the number of accidental pairs with given values of $\Delta {\rm r}_{proj}$ and Δv_n , and thus show what fraction of the structure in Fig. 11 is real. The shaded histograms in Fig. 12 represent the $\Delta {\rm r}_{proj}$ and Δv_n distributions for scrambled versions of the ELG and non-ELG datasets.

In principle, the scrambling of the (r,v)-datasets can be done in three ways. First, one may leave the values of ${\rm r}_{proj}$ and v intact, and only reassign the value of the azimuthal angle of each galaxy randomly. This will keep both the radial density profile as well as the $\sigma_{\rm V}$ -profile intact. However, in that case the galaxies near the centre of a system (with small values of ${\rm r}_{proj}$, and consequently also small values of $\Delta {\rm r}_{proj}$) globally retain their relative velocities, and the scrambling will be far from perfect. Secondly, one may apply velocity scrambling. In that case, the $\sigma_{\rm V}$ -profile is not conserved; however, the average decrease of $\sigma_{\rm V}$ over 1 h^{-1} Mpc is modest (see, e.g. den Hartog and Katgert 1996), and we do not consider the non-conservation of the $\sigma_{\rm V}$ -profile a serious problem.

However, if one does not scramble the azimuthal angle at the same time, velocity scrambling only makes sense if the number of galaxies in a system is quite large. If that is not the case, there will be an important amount of 'memory' between the pairs in the original and in the scrambled data. Therefore, we applied both velocity- and azimuth scrambling. Even then, the scrambled ELG distribution may have significant memory of the observed distribution in view of the small average number of ELG (and therefore ELG-ELG nearest-neighbour pairs) in a system. To minimize this effect (which will lead to an underestimation of the amount of real small-scale structure) we have used for the ELG only the 20 systems with at least 10 ELG (remember that for the non-ELG we used the 75 systems with at least 20 members).

From Fig. 12 we conclude that both for the non-ELG and the ELG there is an excess of nearest-neighbour pairs with $\Delta {\rm r}_{proj} <$ 0.2 h^{-1} Mpc, viz. of about 7% for the non-ELG and about 15% for the ELG. Moreover, for the non-ELG there appears to be a small excess (of about 4%) of nearest-neighbour pairs with $\Delta v_n \lesssim 0.6$. For the ELG the excess is about 7 % , but the values of Δv_n are between ≈ 0.5 and 1.2. The number of excess pairs in the Δv_n distribution is about half that in the $\Delta {\rm r}_{proj}$ distribution, for ELG as well as non-ELG. This must mean that there is more 'memory' about velocity than about position in the scrambled datasets. Nevertheless, it seems safe

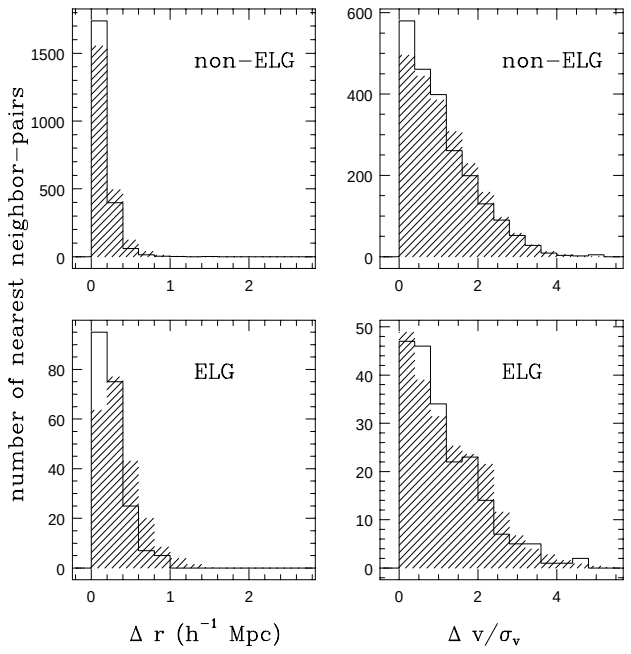

Fig. 12. The observed distributions of Δr_{proj} and $\Delta v/\sigma_{\rm V}$ for all nearest-neighbor pairs of non-ELG (top) and ELG (bottom) are shown as full-drawn line histograms. The shaded histograms represent the same distributions obtained from the observations after scrambling with regard to radial velocity and azimuthal angle (see text for details).

to conclude from Fig. 12 that the ELG show more small-scale structure than the non-ELG. However, whereas the non-ELG excess pairs have small Δr$_{proj}$ as well as small Δv_n , the ELG excess pairs have small Δr$_{proj}$ but fairly large Δv_n 's.

We are thus led to a picture in which a fairly small fraction of the galaxies are in 'real' pairs with small Δr$_{proj}$ and Δv_n , with the fraction of ELG in such pairs probably slightly larger ($\approx$ 20%) than that of non-ELG ($\approx$ 10%). Interestingly, the estimated fraction of ELG in pairs is quite consistent with the value derived in Sect. 4.3. It is a bit puzzling that we now find that the Δv_n 's of these pairs are not very small, whereas in Sect. 4.3 we found that $\sigma_{\rm V}$ for these ELG must be quite small. If one assumes these ELG pairs to be in groups, and if one assumes the relation between the average Δv and $\sigma_{\rm V}$, valid for a gaussian, to hold for those putative groups, one derives typical masses of several times 10^{12} solar masses (using the projected virial mass estimator for isotropic orbits, see Heisler, Tremaine & Bahcall 1985). This implies that the real ELG pairs could be in small groups of a few to several ELG, depending on the average mass of the ELG in question.

6.2. Substructure

It is interesting to find out whether the groups of ELG (and, to a lesser extent, non-ELG) that we 'detected' in the analysis in Sect. 6.1, are detectable as substructure in the velocity-position databases of individual clusters as well. In order to investigate this we have applied the test (due to Dressler & Shectman 1988, but with the modifications proposed by Bird 1994) for the presence of substructure. This test compares the value of a substructure parameter, $\Delta = \sum_{i=1}^{N} \delta_i$, for a cluster, with the distribution of values of the same parameter that one obtains in 1000 Monte Carlo randomizations of the cluster data-set. A large value of δ_i for a given galaxy implies a high probability for it to be located in a spatially compact subsystem, which has either a <v> that differs from the overall cluster mean, or a different $\sigma_{\rm V}$, or both.

Table 6. The Dressler & Shectman test for substructure

name	$< z >$	P$_\Delta$		N,N$_{ELG}$	
		all	non-ELG		
119	0.044	0.620	0.742	101	5
168	0.045	0.324	0.277	76	6
514	0.072	0.017	0.048	81	11
548W	0.042	0.000	0.003	120	24
548E	0.041	0.000	0.003	114	38
978	0.054	0.129	0.071	61	7
2734	0.062	0.063	0.095	77	1
3094	0.068	0.000	0.000	66	16
3112	0.075	0.241	0.688	67	16
3122	0.064	0.005	0.021	89	18
3128	0.060	0.000	0.000	152	30
3158	0.059	0.491	0.218	105	9
3223	0.060	0.179	0.042	73	6
3341	0.038	0.579	0.546	63	11
3354	0.059	0.004	0.000	57	10
3558	0.048	0.247	0.235	73	9
3562	0.048	0.000	0.019	116	21
3651	0.060	0.021	0.061	78	8
3667	0.056	0.212	0.306	103	9
3695	0.089	0.001	0.000	81	9
3744	0.038	0.061	0.025	66	13
3806	0.076	0.078	0.201	97	23
3809	0.062	0.072	0.032	89	21
3822	0.076	0.064	0.053	84	15
3825	0.075	0.072	0.114	59	4

We have applied this test to the 25 systems with $N \geq 50$. These contain a sufficiently large number of galaxies (on average 86 of which 14 are ELG) that for these systems the test may be expected to produce significant results. An additional advantage of this selection is that from all these systems interlopers were removed. In Table 6 we list the probability P$_\Delta$ that a value of Δ as large as the one observed is obtained by chance. When this probability is low, one thus has strong evidence for subclustering. The probability P$_\Delta$ was calculated separately for all galaxies (ELG+non-ELG) (col.3), and for the non-ELG only (col.4), i.e. with the ELG removed.

In 8 systems we find evidence for substructure at the 0.99 conf.level, using all galaxies (i.e. for A548W, A548E, A3094, A3122, A3128, A3354, A3562 and A3695). In addition, there are 2 systems with substructure at the 0.98 conf.level, viz. A514 and A3651. One might suspect that the systems with

a substructure signal are preferentially found among the systems with the largest number of galaxies, as for those it will be relatively easier to detect deviations from uniformity. From Table 6 it indeed appears that there is small effect of this kind: the 8 systems with P_Δ less than 0.01 have an average number of galaxies of 98 ± 13, whereas for the other 17 systems this number is 79 ± 4.

Perhaps more significantly, the 8 systems with signs of substructure have 20 ± 4 ELG, and the other 17 systems only 9 ± 1 ELG on average. This might lead one to suspect that the ELG are a very important, if not *the*, cause of substructure. However, there is no evidence that that is so; among the 8 systems with $P_\Delta < 0.01$ for all galaxies, there are 6 for which P_Δ is still less than 0.01 if the ELG are excluded. Therefore, it is very unlikely that the presence of ELG is a requirement for the occurrence of substructure.

However, there is an indication that the ELG preferentially occur in substructure, if the system to which the ELG belong indeed does have substructure. This presumes that the substructure is probably delineated primarily by the non-ELG (and/or the dark matter), and that the ELG so to speak 'follow' the substructure that is present. This conclusion is based on the following evidence.

Combining all systems with $N \geq 50$, we have compared the distributions of the individual values of δ_i of the 1808 non-ELG and 340 ELG in these 25 systems. According to a KS-test, the probability that the distributions are drawn from the same population is < 0.001. Note that this conclusion does not depend critically on the 8 clusters with clear evidence of substructure. When we exclude these clusters, the δ_i distributions of ELG and non-ELG are still different at the 0.994 conf.level. Using the total sample of galaxies in the 25 clusters, we find that the fraction of ELG is almost twice as large among the galaxies that, according to their value of δ_i, are more likely to reside in substructure, than among the galaxies that are not likely to belong to substructure; $f_{ELG} = 0.15 \pm 0.02$ for galaxies with $\delta_i \geq 2$, and $f_{ELG} = 0.08 \pm 0.02$, for galaxies with $\delta_i \leq 1$.

We conclude therefore that in substructures the ELG occur *relatively* more frequently than the non-ELG. In a fairly small fraction of the systems they may even account for most of the substructure; however, in general the ELG seem to *follow* the substructure rather than that they *define* it. As we saw in Sect. 3.2 there is a clear tendency for the fraction of ELG to be larger in smaller systems. It is thus not totally unexpected to find that the ELG are relatively more associated with substructure since, to some extent, the ELG can be regarded as low-richness groups within richer systems. While ELG are more frequently found in subclusters than non-ELG, their average velocities are seldom different from the cluster ones; therefore, groups containing ELG cannot be rapidly infalling into the cluster, unless the infall of these groups is more or less isotropic.

7. Non-equilibrium and orbits of ELG

For the 75 systems with $N \geq 20$ we have computed the virial and projected masses (see, e.g. Heisler et al. 1985); we have done this for the datasets that include all members as well as for the subsets of non-ELG members. For both mass estimators we find that the estimate based on all the galaxies is 8 % larger than that based on non-ELG only. The distribution of masses computed using only non-ELG is significantly different (at the >0.999 conf.level) from that computed from the combination of non-ELG and ELG.

We have estimated the average ratio of the masses we would have derived separately for ELG and non-ELG. Using an average ELG fraction of 0.15 for the 75 systems used here, we estimate that cluster mass estimates based solely on ELG must, on average, be $\sim$50 % larger than the estimates based on the non-ELG only. Note that this result involves the assumption that ELG and non-ELG have the same type of orbital distribution, so that the same velocity projection factor applies. If the orbital characteristics of ELG and non-ELG are not the same, the difference in the mass estimates may in reality be larger or smaller.

In deriving the difference of 50 % in estimated mass, it has also been tacitly assumed that ELG and non-ELG are both pure categories. However, one must realize (see also Sect. 3.2) that the non-ELG class may harbour a significant contribution of late-type galaxies (about two-thirds of all spirals were not detected as ELG). If the latter share the kinematics of the ELG, there might be an even larger difference between mass estimates based on spiral and non-spiral galaxies.

To forge consistency between the mass estimates based on ELG and non-ELG, the orbits of the non-ELG should be more radial than those of the ELG in order to counteract the lower value of ${\sigma_{\rm V}}^2$ by a larger velocity projection factor. However, this is very unlikely in view of the more centrally concentrated distribution of the non-ELG. Another, more probable solution to the apparent inconsistency between the mass estimates based on ELG and non-ELG is to assume that the ELG are not in equilibrium with the non-ELG. As both classes are in the same potential (to which both probably contribute in a limited way), it would only seem possible for them not to be in equilibrium if they had not adjusted to the potential in the same manner. This could happen if their relaxation times were very different, which in turn could be a natural consequence of the differences in their spatial distribution. As the non-ELG are significantly more concentrated and find themselves in a denser environment, they are more likely to have reached equilibrium than are the ELG.

We have tried to obtain more information on the orbits of ELG and non-ELG by analyzing the dependence on projected radius of the distribution of the line-of-sight component of their velocities. If the statistics of the orbital parameters of ELG and non-ELG are different, their velocity distributions must depend on position in different ways, and that would manifest itself in the distribution of line-of-sight velocities (see e.g. Kent & Gunn 1982, and Merrit 1987).

We have determined the radial dependence of the dispersion of the line-of-sight velocity, using the synthetic cluster formed by adding the 75 systems with at least 20 members. This has the clear advantage of statistical weight but the equally clear

Table 7. The observed radial dependence of σ_V

r_{proj}	number of gals		$\sigma_{V,obs}$	
Mpc	non-ELG	ELG	non-ELG	ELG
< 0.75	2170	310	1.05	1.28
> 0.75	980	239	0.92	1.13
all	3150	549	1.01	1.22

disadvantage of producing an 'average' cluster that may bear little resemblance to any of the real clusters that it is made up of. After clipping of the $> 3\sigma$ outliers this cluster contains 3699 galaxies of which 549 are ELG. In Table 7 we show the values of σ_V for two radial bins as well as the overall value, for ELG and non-ELG. The bins have been chosen as a compromise between optimizing the detection probability for orbital anisotropy, if it exists, and the statistical weight for its detection. E.g., decreasing the size of the inner bin increases the discrimating power for orbital anisotropy, but decreases the statistical weight for its detection.

In adding the data for the 75 systems, the values of r_{proj} have not been scaled but the velocities have been scaled with the global value of σ_V of each cluster. The values of σ_V in Table 7 are thus in units of the overall σ_V of the synthetic cluster. One might wonder why σ_V of the non-ELG is larger, instead of smaller, than 1.00 (after all, the combination of ELG and non-ELG should give σ_V exactly equal to 1.00). The reason is that, in adding many normalized guassians, the errors in the means of the individual guassians produce an overall sigma that is slightly larger than 1.00.

The Table confirms the large difference between ELG and non-ELG as regards overall σ_V and, at the same time, shows that the ratios of the σ_V 's in the inner and outer bin are remarkably similar (viz. 1.14 and 1.13) for ELG and non-ELG. The first impression could be that this indicates similar orbits for ELG and non-ELG. However, that cannot be the case, as the density distributions of ELG and non-ELG are significantly different.

From some fairly simple modeling, we have predicted values of σ_V for ELG and non-ELG in the two radial bins defined in Table 7. We used a model with 3 - D density profiles described by β-models with a β of -0.71, and r_c's of 0.15 and 0.42 h^{-1} Mpc for non-ELG and ELG respectively, i.e the values we found from the fits to the surface density profiles (see Sect. 5). In addition, we specify a velocity distribution at each position that is described by a value for the velocity dispersion in the radial direction, $\sigma_{rad}(r)$, and a constant anisotropy parameter $\mathscr{A}$ (= 1–$(\sigma_{tan}/\sigma_{rad})^2$). The value of $\sigma_{rad}(r)$ was assumed to depend linearly on radius, viz. $\sigma_{rad}(r) = \sigma_{rad}(0) - \varpi\ r$.

From the 3-D density profile, we randomly extract 10^5 points. Since our clusters are sampled to different limiting radii, the total sample including all clusters is not complete at large distances from the center. To mimic this incompleteness in our simulated sample, we did not include the simulated points with $r_{proj} > 1.2\ h^{-1}$ Mpc . From Table 1 is can be seen that the median of the largest r_{proj} in the clusters is essentially 1.2 h^{-1} Mpc . We included all points with $r_{proj} < 1.2\ h^{-1}$ Mpc as long as the 3 - D clustercentric distance was less than 10 h^{-1} Mpc . In this manner, we reproduced to within a few percent the observed fractions of galaxies in the inner and outer bins, for ELG as well as non-ELG.

For each of the simulated points, we randomly extracted three velocity components from three gaussian velocity distributions that follow from the velocity dispersion profile and the anisotropy. We assumed the two components in the tangential directions to have the same dispersion, which follows from σ_{rad} and $\mathscr{A}$. We then projected the velocity vector along the line-of-sight, and added noise to the resulting line-of-sight velocity by adding two random deviates. The first simulates the errors in the individual velocity measurements (assumed to be 0.1 σ_V), the other the error in the average cluster velocity (assumed to be 0.2 σ_V). Finally, as in the observations, we rejected all simulated (line-of-sight) velocities outside $\pm 3\sigma$.

The model parameter were optimized as follows. First, we estimated the best values of $\sigma_{rad}(0)$ and ϖ for the non-ELG, assuming the orbits to be isotropic, i.e. $\mathscr{A} \equiv 0.0$. In order to reproduce the observed values of σ_V for the non-ELG we need $\sigma_{rad}(0) = 1.13$ and $\varpi = -0.14$. This implies that σ_{rad} decreases to zero at a radial distance of 8.1 Mpc, which is quite acceptable in view of the expected turn-around radius of the 'synthetic' cluster. This model produces inner and outer σ_V 's for the non-ELG of 1.05 and 0.92 respectively, i.e. exactly as observed.

Next, we tried to model the observed σ_V values of the ELG, again assuming isotropic orbits. We have no prescribed relation between the $\sigma_{rad}(0)$'s of ELG and non-ELG, except that it is very hard, if not impossible, to imagine that the ratio of the $\sigma_{rad}(0)$'s for ELG and non-ELG could exceed $\sqrt{2}$. The best value of $\sigma_{rad}(0)$ for the ELG was found to be 1.50, which then implies a value $\varpi = -0.19$ (because we assume that the radius at which σ_{rad} decreases to zero is the same for ELG and non-ELG). This model does not do a very bad job, but it does not fully reproduce the decrease of σ_V from the inner to the outer bin. One way to improve the agreement between model and observations would be to assume a larger value for ϖ for the ELG than for the non-ELG. Although we cannot totally exclude the possibility that the ELG have a steeper velocity dispersion profile than the non-ELG, the data that we have for the inner part of the 'synthetic' cluster do not indicate this (see also below).

Another way to improve the agreement between observed and predicted σ_V 's of the ELG is to assume that the velocity distribution of the ELG is anisotropic; in other words: to assume that the anisotropy parameter $\mathscr{A} \neq 0$. In that case there are two free parameters: $\sigma_{rad}(0)$ and $\mathscr{A}$; the value of ϖ will follow directly from $\sigma_{rad}(0)$ and the maximum radius of 8.1 Mpc found for the non-ELG. The best solution has to be determined by iteration because the observed global value of σ_V does not, for a given value of $\mathscr{A}$ (assumed to be independent of radial distance), immediately yield the value of $\sigma_{rad}(0)$. If σ_{1d} had been derived in an aperture with sufficiently large projected radius, *and* if $\varpi = 0$, $\sigma_{rad}(0)$ would have followed directly as $\sqrt{3/(3 - 2 \times \mathscr{A})} \times \sigma_{1d}$. As neither of these two conditions

Table 8. The modeled radial dependence of σ_V

	non-ELG		ELG							
	obs	model	obs	model						
$\mathscr{A}$		0		0	-0.9	-0.6	-0.3	0.3	0.6	0.9
$\sigma_{rad}(0)$		1.13		1.50	1.25	1.31	1.38	1.64	1.86	2.34
ϖ		-0.14		-0.19	-0.16	-0.16	-0.17	-0.21	-0.23	-0.29
< 0.75	1.05	1.05	1.28	1.26	1.25	1.25	1.25	1.26	1.27	1.28
> 0.75	0.92	0.92	1.13	1.17	1.19	1.18	1.17	1.17	1.15	1.13
all	1.01	1.01	1.22	1.22	1.22	1.22	1.22	1.22	1.22	1.22

is fulfilled, we had to iteratively find the best combination of $\sigma_{rad}(0)$ and ϖ for each value of $\mathscr{A}$ that we assumed.

In Table 8 we summarize the results of the modeling, for non-ELG as well as ELG. It can be seen that models with $(\sigma_{tan}/\sigma_{rad}) > 1.0$ (i.e $\mathscr{A} < 0$) predict that the observed dispersion of the line-of-sight velocity component does not decrease sufficiently with r_{proj}. This was to be expected since we needed the anisotropy to increase the ratio between the inner and outer values of σ_V of the ELG, but that can only be accomplished with radially elongated orbits.

The most probable value of $\mathscr{A}$ for the ELG is not very well determined from our data, because the uncertainties in the observed inner and outer values of σ_V for the ELG are estimated to be 4–5%. However, taking the data at face-value we conclude that the best fit is obtained for $\mathscr{A} \approx 0.9$, but a value of 0.3, or even 0.0 cannot be formally exluded. On the contrary, we think that negative values of $\mathscr{A}$ can be fairly safely ruled out. From Table 8 we therefore conclude that $\mathscr{A} \approx 0.5 \pm 0.5$, which thus provides some evidence for anisotropy of the ELG orbits but not very strong evidence.

We think that the evidence for anisotropy of the ELG orbits is, in fact, quite a bit stronger if one considers not just the inner and outer values of σ_V but includes the total velocity dispersion profile. In Fig. 13 we show the observed velocity dispersion profiles for the non-ELG (upper panel) and the ELG (solid lines in the lower panel) in the synthetic cluster. The σ_V profiles were derived with the LOWESS method (Gebhardt et al. 1994). The heavy lines represent the observed σ_V , the two thin lines on either side indicate the 95% confidence bands, obtained from 1000 Monte Carlo simulations of the dataset (for details, see e.g. Gebhardt et al.) The increase of the uncertainty in the estimate of the ELG σ_V for $r_{proj} \lesssim 0.3 h^{-1}$ Mpc is due to the flat ELG surface-density profile. It must be realized that the values in Table 8 are weighted averages over the indicated intervals, where the weights follow from the observed surface densities shown in Fig. 10. In the lower panel we also show the predicted velocity dispersion profiles of ELG for three models, viz. those with $\mathscr{A}$ = -0.6, 0.0 and 0.6

On the basis of the steep gradient of the ELG σ_V within 1.0 h^{-1} Mpc , we consider it quite unlikely that for the ELG the value of $\mathscr{A}$ is practically 0.0 (i.e. that the ELG orbits are isotropic). Instead, the sharp increase of the ELG σ_V within 1.0 h^{-1} Mpc is produced by galaxies that mostly are at quite some distance from the centre where, in our model, σ_{rad} has already decreased considerably from its central value $\sigma_{rad}(0)$. To produce the observed values of the line-of-sight velocity dispersion would seem to require inevitably that the line-of-sight velocity component is significanty 'boosted' by radial anisotropy. Combining the data in Table 8 and the information in Fig. 13, we conclude that the best estimate for $\mathscr{A}$ is probably $\approx 0.6 \pm 0.3$ which implies a value for $\sigma_{tan}/\sigma_{rad}$ between $\approx$0.3 and 0.8. Note that we have not given much weight to the data within $0.3 h^{-1}$ Mpc due to their large uncertainty. Had we given those more weight, we would have arrived at a lower value of $\mathscr{A}$, probably between 0.0 and 0.3. However, for those values of $\mathscr{A}$ the predicted velocity dispersion profile seems to give a rather bad representation of the observed slope between 0.3 and $1.0 h^{-1}$ Mpc .

As mentioned before, the shape of the *full distribution* of line-of-sight velocities (rather than only the dispersion) at different r_{proj} could, in principle, provide information on the orbits. However, we have calculated those distributions for the models summarized in Table 8 and found that with our statistics the shapes are not a sufficiently sensitive discriminant.

8. Discussion and conclusions

Our study of the properties of emission-line galaxies in clusters has yielded several results which we will now try and put together into a more or less coherent picture. Some results are not unexpected and confirm earlier results by other authors. On the other hand, we also obtained some results that are totally new (among which the analysis of the ELG orbits), and which are based on a sample of many tens of rich clusters. Thereby our data provide evidence for the general occurence of dynamical effects that up to now were seen only in one or two individual clusters.

In the following discussion it must always be clearly realized that our ELG simply are galaxies that had *detectable* emission lines in the ENACS spectra. In several instances we will think of them as (mostly late-type) spirals. This is justified as we found (for a subset) that *well over 90% of them were classified as spirals*. However, they represent *only about 1/3 of the* **total** *spiral population*, as a result of our observational limit, and the variation in gas content of spirals of different types. When comparing the ELG with the non-ELG, we are thus always comparing a very

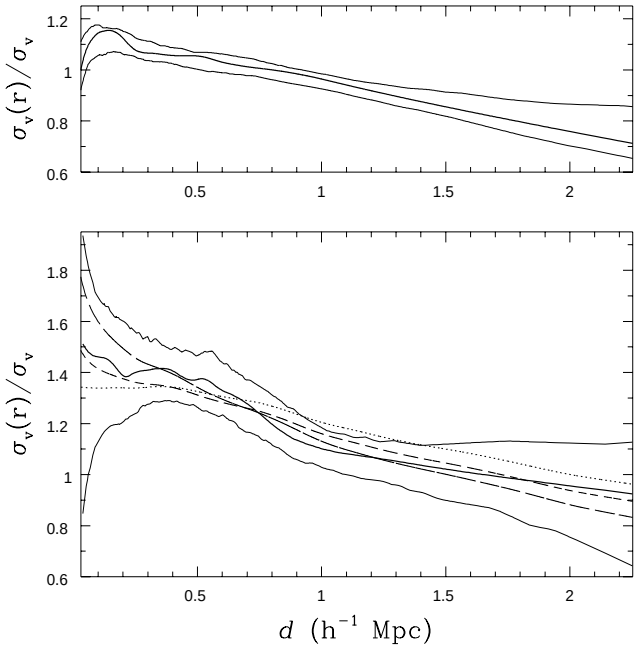

Fig. 13. The velocity-dispersion profiles for non-ELG (upper panel) and ELG (lower panel) in the synthetic cluster. The full-drawn curves refer to the data, with heavy lines representing the observed profiles while the thin lines indicate the 95% confidence limits. In the lower panel, three model predictions for different values of the anisotropy parameter $\mathscr{A}$ are given, viz. $\mathscr{A}$ = -0.6 (dotted), 0.0 (short dashes) and 0.6(long dashes).

homogeneous class (ELG; read: spirals) with a heterogeneous class consisting of both non-spirals (ellipticals and SO's) and spirals.

The most striking results that we obtained concern the spatial distribution and the kinematics of the ELG, especially when compared with those of the non-ELG.

First, the ELG very clearly avoid the central regions of clusters, and the difference in central concentration of ELG and non-ELG probably implies an even larger difference in the central concentration of spirals and non-spirals. In the cluster Abell 576, Mohr et al. (1996) recently also found a clear deficit of ELG in the central region. The different spatial distributions are totally consistent with the well-documented dependence of the mix of early- and late-type galaxies on local galaxy density. The clear dependence of the fraction of ELG on the global σ_V of a cluster that we found can easily be understood as a manifestation of this dependence. Several physical mechanisms have been proposed for the dependence of galaxy mix on local density. We will argue below that the kinematics of the ELG make it likely that they still contain gas that produces detectable emission lines because they have not yet been inside the high-density central cluster region.

The characteristic of the kinematics of the ELG that supports this explanation most convincingly is their high velocity dispersion. For the reasons explained above, we expect the observed ratio of the σ_V 's of ELG and non-ELG of $\approx$1.2 to translate into a larger σ_V ratio for spirals and non-spirals. In this respect it is noteworthy that Colless & Dunn (1996) find that σ_V of the late-type galaxies in the main concentration in the Coma cluster is very close to $\sqrt{2}$ times that of the early-type galaxies, which they interpret as suggesting that the late-type galaxies are freely falling into the cluster core.

Since we applied an interloper removal criterion irrespective of whether a galaxy was classified as ELG or non-ELG, all our ELG (including those projected onto the cluster core) are cluster members, i.e. are within the present turn-around radius of their cluster. We expect therefore that, had we been able to compare σ_V of the spirals with that of the early-type non-ELG (i.e. excluding the non-ELG spirals) we would have obtained the same result as did Colless & Dunn.

Our result of a systematically larger σ_V for ELG than for non-ELG (which is based on an ensemble of many clusters) is supported by recent observations of some individual clusters; Mohr et al. (ibid.) find a similar effect in Abell 576, and Carlberg et al. (1996) conclude for a sample of about 15 clusters with redshifts between 0.15 and 0.55 that '... the bluer galaxies, which often contain measurable emission lines, statistically are found to have a higher velocity dispersion than the redder absorption line galaxies, an effect that is particularly prominent near the projected center of the cluster ...'.

We believe that the larger σ_V of ELG (and of the spirals) is a generic aspect of the dynamics of galaxy clusters. It probably indicates that the spirals that we see today avoid the central regions because they either have not yet got there (the free-fall time is certainly not much shorter than the Hubble time), or have passed by the core on orbits that did not traverse the very dense central region. In other words: the dynamical state of the ELG reflects the phase of fairly ordered infall (of spirals) rather than the virialized condition in the relaxed core, the size of which is probably only $\approx$0.5 h^{-1} Mpc (e.g. den Hartog and Katgert 1996).

In this picture, the orbits of the ELG (and therefore of the spirals) are expected to be fairly radial, and their velocity distribution is expected to be quite anisotropic. The statistical weight of our synthetic cluster with 549 ELG has allowed, we think for the first time, a meaningful check of this prediction to be made. The uncertainties of the ratio of the inner and outer σ_V 's still prevent the anisotropy parameter $\mathscr{A}$ to be solved for with high precision. However, the strong rise of σ_V of the ELG towards the centre, which was also seen by Mohr et al. in Abell 576 and by Carlberg et al. (see above), quite strongly supports the notion of predominantly radial orbits of at least the ELG that are projected onto the central region.

A moderate to fairly strong anisotropy of the velocity distribution of the ELG can also solve the apparent discrepancy of the mass estimates based on ELG and non-ELG. We do not have a very accurate estimate of the magnitude of the discrepancy because the non-ELG category does contain spirals. Yet, the mass derived from spirals will (in terms of the mass indicated by the non-spirals) be at least as large as that derived from the ELG compared to the mass of the non-ELG, unless the kinematics of the non-ELG spirals is totally different from that of the ELG.

From the discussion in Sect. 7, we estimate a discrepancy of at least a factor 1.5. In the projected mass estimator

$$M_{PM} = \frac{f_{PM}}{GN} \sum_i v_{1di}^2 r_{\perp i} \quad (3)$$

where N is the number of galaxies in the system, v_{1di} the observed velocity along the line-of-sight, and $r_{\perp i}$ the projected clustercentric distance of the $i-th$ galaxy (Heisler et al. 1985), the factor f_{PM} is a projection factor that depends on the distribution of orbits. It is equal to $64/\pi$ and $32/\pi$ for the cases of radial ($\mathscr{A} = 1$) and isotropic ($\mathscr{A} = 0$) orbits, respectively. More generally, one can show that

$$f_{PM} = \frac{4 - 2\mathscr{A}}{4 - 3\mathscr{A}} \frac{32}{\pi} = f(\mathscr{A}) \frac{32}{\pi} \quad (4)$$

where the anisotropy parameter $\mathscr{A}$ is assumed constant throughout the system (see also Perea et al. 1990). If the ELG indeed are not in equilibrium with the relaxed core, the mass estimate based on them could be twice as large as the one based on the other galaxies. This means that f($\mathscr{A}$) may be as large as 4/3, which implies that $\mathscr{A}$ may be as large as 0.7, which is consistent with the best value for $\mathscr{A}$ derived in Sect. 7.

The assumption that the spirals that we observe today are mostly falling in for the first time is also consistent with the fact that, contrary to earlier claims, we do not see any need for different emission-line properties of ELG in clusters and ELG in the field. In this respect it is noteworthy that only a fairly small fraction of the ELG occur in compact subgroups. Our data are thus consistent with a picture in which the infall of the spirals is rather isotropic. Whether this is indeed so, or an artefact of our analysis, in which we combined many clusters most of which contain only a fairly small number of ELG, will become clear as soon as the results from the more extensive multi-object cluster spectroscopy, that is presently under way, will become available.

Acknowledgements. It is a pleasure to thank Tim Beers, Gigi Fasano and Karl Gebhardt who kindly provided us with Fortran codes for the evaluation of robust statistics (*ROSTAT*), the 2-D KS-test, and the evaluation of the velocity dispersion profiles (*LOWESS*), respectively, and Alan Dressler for kindly providing us with an electronic copy of his data-set on cluster galaxy morphologies.

AB and PK thank Walter Jaffe for asking helpful questions about the modelling. AM acknowledges financial support from the French GDR Cosmologie and INSU; JP acknowledges support from the Spanish DGICYT (program PB93-0159); and PF acknowledges support from the Italian MURST.

References

Abell G.O., Corwin H.G., Olowin R.P., 1989, ApJS 70, 1
Andreon S., 1993, A&A 276, L17
Andreon S., 1994, A&A 284, 801
Beers T.C., Flynn K., Gebhardt K., 1990, AJ 100, 32
Beers T.C., Tonry J.L., 1986, ApJ 300, 557
Binggeli B., Tammann G.A., Sandage A., 1987, AJ, 94, 251
Binggeli B., Tarenghi M., Sandage A., 1990, A&A 228, 42
Bird C.M., 1994, AJ 107, 1637
Biviano A., Girardi M., Giuricin G., Mardirossian F., Mezzetti M., 1992, ApJ 396, 35
Carlberg R.G., Yee H.K., Ellingson E., et al., 1996, ApJ 462, 32
Colless M., Dunn A.M., 1996, ApJ 458, 435
Davis D., Bird C., Mushotky R., Odewahn S., 1995, ApJ 440, 48
den Hartog R., Katgert P., 1996, MNRAS 279, 349
de Vaucouleurs G., 1961, ApJS 6, 213
Dressler A., 1980a, ApJ 236, 351
Dressler A., 1980b, ApJS 42, 565
Dressler A., Shectman S.A., 1988, AJ 95, 985
Dressler A., Thompson I.B., Shectman S.A., 1985, ApJ 288, 481
Escalera E., Biviano A., Girardi M., et al., 1994, ApJ 423, 539
Fasano G., Franceschini A., 1987, MNRAS 225, 155
Gebhardt K., Pryor C., Williams T.B., Hesser J.E., 1994, AJ 107, 6
Girardi M., Biviano A., Giuricin G., Mardirossian F., Mezzetti M., 1995, ApJ 438, 527
Gisler G.R., 1978, MNRAS 183, 633
Gunn J.E., Gott J.R., 1972, ApJ 176, 1
Heisler J., Tremaine S., Bahcall J.N., 1985, ApJ 298, 8
Hill J.M., Oegerle W.R., 1993, AJ 106, 831
Hubble E., Humason M.L., 1931, ApJ 74, 43
Iovino A., Giovanelli R., Haynes M., Chincarini G., Guzzo L., 1993, MNRAS 265, 21
Katgert P., Mazure A., Perea J., et al., 1996, A&A 310, 8 (Paper I)
Kent S.M., Gunn J.E., 1982, AJ 87, 945
Lubin L.M., Bahcall N.A., 1993, ApJ 415, L17
Mazure A., Katgert P., den Hartog R. et al., 1996, A&A 310, 31 (Paper II)
Merritt D., 1987, ApJ 313, 121
Merritt D., Gebhardt K., 1994, in "Clusters of Galaxies", p.11, F. Durret, A. Mazure, J. Trân Thanh Vân eds., Editions Frontières, Gyf-sur-Yvette, France
Mohr J.J., Geller M.J., Fabricant D.G., et al., 1996, ApJ 470, 724
Moss C., Dickens R.J., 1977, MNRAS 178, 701
Oemler A., 1974, ApJ 170, 241
Osterbrock D.E., 1960, ApJ 132, 325
Perea J., del Olmo A., Moles M., 1990, A&A 237, 319
Press W.H., Flannery B.P., Teukolsky S.A., Vetterling W.T., 1986, Numerical Recipes – The Art of Scientific Computing, Cambridge University Press, Cambridge, UK.
Salzer J.J., MacAlpine G.M., Boroson T.A., 1989, ApJS 70, 479
Salzer J.J., Moody J.W., Rosenberg J.L., Gregory S.A., Newberry M.V., 1995, AJ 109, 2376
Sanromà M., Salvador-Solé E., 1990, ApJ 360, 16
Sarazin C.L., 1986, Rev. Mod. Phys. 58, 1
Sodré L., Capelato H.V., Steiner J.E., Mazure A., 1989, AJ 97, 1279
Tammann G.A., 1972, A&A 21, 355
Tully R.B., Shaya E.J., 1984, ApJ 281, 31
van den Bergh S., 1962, AJ 67, 285
van Haarlem M., van de Weygaert R., 1993, ApJ 418, 544
Yahil A., Vidal N., 1977, ApJ 214, 347
Yepes G., Dominguez-Tenreiro R., del Pozo-Sanz R., 1991, ApJ 373, 336
Zabludoff A.I., Franx M., 1993, AJ 106, 1314
Zucca E., Vettolani G., Cappi A. et al., 1995, to appear in Astrophysical Letters & Communications, proceedings of the workshop "Observational Cosmology: from Galaxies to Galaxy Systems", Sesto, Italy, 4–7 July 1995

This article was processed by the author using Springer-Verlag LaTeX A&A style file *L-AA* version 3.